

# Łukasz Cywiński - self report

## 1 Personal data

Łukasz Cywiński

## 2 Education and degrees

- Ph.D. student in Physics, University of California, San Diego. Thesis defended on June 12th 2007. Title of the dissertation: *Magnetization Dynamics and Spin Diffusion in Semiconductors and Metals*.  
Advisor: professor Lu Jeu Sham.
- M. Sc. in Physics, Warsaw University, Poland, 19th June 2002.  
Title of thesis: *Wpływ nieporządku i swobodnych nośników na absorpcję międzypasmową w półprzewodnikach (Influence of disorder and free carriers on interband absorption in semiconductors)*.  
Advisor: prof. dr hab. Witold Bardyszewski.

## 3 Information on previous employment

- 04/2009– present: Adjunct in the Laboratory for Cryogenic and Spintronic Research, group of spin phenomena physics SL2.2, in the Institute of Physics, Polish Academy of Science, Warsaw.
- 2007-2009: Post-doctoral Research Associate at Condensed Matter Theory Center, University of Maryland, College Park.
- 2002-2007: Graduate student in Physics, University of California, San Diego

## 4 Scientific achievement being the basis of the habilitation procedure

The scientific achievement, in accordance with the art. 16 paragraph 2 of the Act of March 14th, 2003, concerning the scientific degrees and titles (Dz. U. no. 65, item 595, as amended), is the series of publications entitled:

a) “Theory of decoherence of solid-state based qubits”.

b) The list of publications constituting the scientific achievement:

- H1. Ł. Cywiński, R.M. Lutchyn, C.P. Nave, and S. Das Sarma, *How to enhance dephasing time in superconducting qubits*, Phys. Rev. B **77**, 174509 (2008)
- H2. Ł. Cywiński, W.M. Witzel, and S. Das Sarma, *Electron Spin Dephasing due to Hyperfine Interactions with a Nuclear Spin Bath*, Phys. Rev. Lett. **102**, 057601 (2009).
- H3. Ł. Cywiński, W.M. Witzel, and S. Das Sarma, *Pure quantum dephasing of a solid state electron spin qubit in a large nuclear spin bath coupled by long-range hyperfine-mediated interactions*, Phys. Rev. B **79**, 245314 (2009).
- H4. Ł. Cywiński, V.V. Dobrovitski, and S. Das Sarma, *Spin echo decay at low magnetic fields in a nuclear spin bath*, Phys. Rev. B **82**, 035315 (2010).

- H5. Ł. Cywiński, *Dephasing of electron spin qubits due to their interaction with nuclei in quantum dots*, Acta Phys. Pol. A **119**, 576 (2011).
- H6. E. Barnes, Ł. Cywiński, and S. Das Sarma, *Master equation approach to the central spin decoherence problem: Uniform coupling model and role of projection operators*, Phys. Rev. B **84**, 155315 (2011).
- H7. J.-T. Hung, Ł. Cywiński, X. Hu, and S. Das Sarma, *Hyperfine interaction induced dephasing of coupled spin qubits in semiconductor double quantum dots*, Phys. Rev. B **88**, 085314 (2013).
- H8. Ł. Cywiński, *Dynamical decoupling noise spectroscopy at an optimal working point of a qubit*, Phys. Rev. A **90**, 042307 (2014).

c) **Description of the scientific goal and the obtained results contained in a monothematic group of research papers presented here as a scientific achievement**

#### 4.1 Introduction and motivation

About 20 years ago the experimental research on truly quantum properties of matter entered a new era, in which the coherent manipulation and measurement of individual quantum systems became possible. The mid-90s breakthroughs in manipulation of quantum states of single trapped ions [1] and of small numbers of microwave radiation photons trapped in a cavity [2] were recognized in 2012 by the Nobel committee. In the context of this dissertation it is important to note that these pioneering experiments also demonstrated how interaction with an environment leads to decoherence of quantum states of a single system [3].

At the same time interest in creation of a quantum computer was spurred by two theoretical breakthroughs: the discovery of quantum algorithm of factorization by Shor [4], and the proof of possibility of error correction of quantum states of qubits [5]. These provided both the strong practical motivation and the hope for actually achieving the goal of building a large-scale (multi-qubit) device exhibiting quantum coherence.

The resulting excitement quickly affected the community of solid state physicists. Since the classical computation is the main area of practical application of solid state physics (especially semiconductor physics), it was natural to suggest to build a quantum computer with solid-state devices. The most often invoked motivation was the prospect of easy scalability of such a system (something which is not obvious with, say, trapped ions). The main obstacle in this endeavour is the fact that, in contrast to the systems studied in quantum optics, the semiconductor or superconductor based qubits are embedded in a condensed matter environment. Strong coupling with many environmental degrees of freedom (lattice vibrations, fluctuating electric fields due to moving charges, magnetic field fluctuations due to paramagnetic spins present in the material, etc.) means that the decoherence is expected to be much faster.

The question of whether the benefits of potential scalability outweigh the drawbacks associated with the strong coupling to nontrivial environment remains still unsettled. However, from the point of view of basic science, the research on solid-state based qubits during the last 15 years has been quite fascinating. Most importantly in the context of this dissertation, the strong coupling to an environment having rich physics can be seen as an interesting theoretical challenge, which requires going beyond the weak-coupling and Markovian approximations.

The research described below encompasses two facets of the decoherence problem for the solid-state based qubits. In chapter 4.2 I will review the theory of decoherence of a spin qubit (a spin of an electron localized in a semiconductor quantum dot) which is interacting via hyperfine coupling with the spins of the nuclei of atoms of the host material. In this case the Hamiltonian of the environment and of the qubit-environment coupling is known (thanks to previous theoretical and experimental studies), and the theoretical challenge is posed by the strong qubit-bath coupling

and the slowness of the dynamics of the environment. These two preclude the use of Born-Markov approximation (which leads to textbook Bloch-Redfield equations for Markovian dynamics of the qubit's reduced density matrix). In chapter 4.3 I will focus on an often encountered (in condensed matter systems) situation, in which the information on the dominant source of noise affecting the qubit is lacking. Either the main source of noise is simply unknown, or important parameters characterizing the environment are not available from measurements other than those of the qubit itself. I will discuss there how, under the assumption that the bath is a source of classical Gaussian noise, one can use the measurements of coherence dynamics to reconstruct the spectral density of such a noise. The two parts of the dissertation are therefore complementary, but it should be noticed that the calculations from section 4.3.2, where qubit coupling to a square of noise is considered, have a similarity to the theory of hyperfine-induced decoherence of electron spin from section 4.2.4. This similarity is not accidental: below I will try to explain how the interaction with the nuclear bath can be approximately mapped on the problem of quadratic coupling to a Gaussian-distributed quantum variable.

## 4.2 From the microscopic description of the environment to calculation of qubit's decoherence dynamics: the case of electron spin coupled to the nuclear bath

In this chapter I will describe a theory of decoherence of a single localized electron spin caused by its interaction with a bath of nuclear spins. Creation of this theory was motivated by spin echo experiments on quantum-dot based spin qubits which were conducted between 2005 and 2008, especially Refs. [6, 7]. At that time no existing theoretical model was applicable to the regime of rather low magnetic fields in which these experiments were conducted. The theory presented in papers [H2] and [H3] was focused on this regime in quantum dots based on III-V compound semiconductors. The formalism presented in these articles allowed for efficient calculation of the spin echo signal, and it was used to predict coherence dynamics in other experimental protocols. The predictions of papers [H2,H3] for the case of spin echo were later confirmed by experiments [8]. Furthermore, while the Ring Diagram Theory (RDT) of [H2,H3] was relying on the assumption of large nuclear bath (technically it employed  $1/N$  expansion, where  $N$  is the number of nuclei appreciably coupled to the electron spin), the comparison of RDT with exact numerical simulations of a system with  $N = 20$  spins [H4] showed that it can describe quite well the spin echo decay due to interaction with such a rather small environment. These results were discussed in a review paper [H5], where the close relation between the RDT at short times and calculation using the quasi-static bath approximation was noted.

The RDT of Refs. [H2,H3] employs an effective pure-dephasing Hamiltonian obtained from the full Hamiltonian of the hyperfine interaction by an approximate canonical transformation. Such an approach can be straightforwardly generalized to more complicated multi-electron systems. The most important example of such a system is a singlet-triplet (S-T) qubit in a double quantum dot, which has been a subject of intense experimental research since 2005 [6, 8–10]. The effective Hamiltonian based calculation of singlet-triplet decoherence is the subject of paper [H7], where predictions for coherence decay are given for the S-T qubit operated in the regime of singlet-triplet splitting larger than the typical Overhauser splitting of two-electron spin states.

Despite the fact that the RDT successfully predicted the spin echo decay at low magnetic fields in GaAs, doubts about the validity of the effective Hamiltonian approach were raised in works in which the Nakajima-Zwanzig (NZ) generalized Master equation approach was employed while using the full hyperfine Hamiltonian [11, 12]. The paper [H6] sheds some light on the relation between the effective-Hamiltonian approach of [H2,H3] and the results obtained using the NZ approach.

The first three sections of this chapter contain a rather detailed review of the physics of spin qubits interacting with the nuclear bath. I hope that they provide enough background for the subsequent three sections, in which the results of papers [H2-H7] are summarized.

### 4.2.1 Semiconductor spin qubits and the nuclear bath

When using a spin of a single electron confined in a quantum dot (QD) as a qubit was proposed in 1998 [13], quantum dots available then had at least tens of electrons confined in them, and there was in fact no truly realistic idea for readout of single-spin states. Work done during the subsequent decade changed this, and by about 2006 qubits based on single spins, and pairs of spins in double dots, were initialized, coherently controlled, and read-out in many laboratories. Spins confined in electrostatically defined gated quantum dots in GaAs were controlled with time-dependent gate voltages [14], while the ones confined in self-assembled InGaAs quantum dots were controlled optically [15, 16]. In the following we will take the coherent control of spin for granted, since we focus here on the interaction of the spin with its environment and the resulting decoherence of quantum states of the qubit.

Before a single spin was actually confined in a quantum dot, it was predicted that its energy relaxation in finite magnetic field  $B$  (longitudinal relaxation in the NMR/ESR terminology) will be dominated by processes of phonon scattering, with the spin-orbit interaction allowing for transitions between the Zeeman-split energy levels [17] (see also [14] for a very transparent discussion). This prediction was experimentally verified in both self-assembled [18] and gated QDs [19], with the phonon-induced processes identified by their characteristic  $B$  and temperature dependence. The phonon-induced energy relaxation could be described using the standard Bloch-Redfield [20] approach: the spin-phonon coupling is weak, allowing for using the second-order perturbation theory, and the autocorrelation time of the phonon bath is much shorter than the timescale on which the spin relaxes, allowing for the use of Markovian approximation leading to the exponential decay of the elements of qubit's reduced density matrix. It is also important to note that the relaxation times  $T_1$  are at least a millisecond for typical experimental conditions. The phonon contribution to spin dephasing (transverse relaxation in the NMR/ESR terminology) was theoretically shown [21] to lead to dephasing time  $T_2 = 2T_1$ , showing that if the lattice vibrations and spin-orbit coupling were the main source of decoherence, spin qubits would remain coherent for up to a millisecond. Unfortunately, it is not the phonon bath that is the most dangerous for spins in semiconductors. The main culprit demanded the development of theoretical methods more complicated and interesting than the textbook Bloch-Redfield theory.

#### *The hyperfine coupling of the electron spin to the nuclear spins and the nuclear Hamiltonian.*

Already around 2001 it was noticed that the most dangerous environment affecting the coherence of a spin localized in a semiconductor is in fact the bath of nuclear spins coupled to the electron by contact hyperfine (hf) interaction [22–24]. This is especially relevant for III-V materials such as GaAs and InGaAs, since neither Ga, nor In and As have any zero-spin isotopes. In the following I will focus on the case of III-V quantum dots, but it should be kept in mind that the spin bath is almost ubiquitous in the case of semiconductor spin qubits (also the ones in silicon and diamond), and for all the single-spin qubits being currently investigated it is the main source of decoherence.<sup>1</sup>

The hf coupling of a localized electron spin to nuclear spins is described by the Hamiltonian

$$\hat{H}_{\text{hf}} = \sum_i A_i \hat{\mathbf{S}} \cdot \hat{\mathbf{J}}_i, \quad (1)$$

where  $\hat{\mathbf{S}}$  is the electron spin operator,  $\hat{\mathbf{J}}_i$  is the operator of the  $i$ -th nuclear spin, and the contact hf couplings  $A_i = \mathcal{A}_{\alpha[i]} |\Psi(\mathbf{r}_i)|^2$ , where  $\Psi(\mathbf{r}_i)$  is the electron envelope function at the  $i$ -th nuclear site (with normalization to the primitive unit cell volume:  $\int_V |\Psi(\mathbf{r})|^2 d\mathbf{r} = \nu_0$ ). The hf energies

---

<sup>1</sup>In the case of qubits based on more than one spin, such as the singlet-triplet qubit, the manipulation of which relies on exchange interaction between the two electrons, the charge noise might be in fact more important in some parameter regimes [25]. In any case, it is easier to suppress charge noise than remove the nuclear spins from a typical semiconductor nanostructure.

$\mathcal{A}_\alpha$  for a nuclear species  $\alpha$  are  $\mathcal{A}_\alpha = \frac{2}{3}\mu_0\hbar^2\gamma_S\gamma_{J\alpha}|u_\alpha|^2$ , where  $\mu_0$  is the vacuum permeability,  $\gamma_S$  and  $\gamma_{J\alpha}$  are the electron and nuclear spin gyromagnetic factors, respectively, and  $u_\alpha$  is the amplitude of the periodic part of the Bloch function at the position of the nucleus of  $\alpha$  species (the normalization is  $\int_{\nu_0} |u(\mathbf{r})|^2 d\mathbf{r} = 1$ ). The number of nuclei interacting appreciably with the electron is defined as

$$N \equiv \frac{\int |\Psi(\mathbf{r})|^2 d^3r}{\int |\Psi(\mathbf{r})|^4 d^3r}, \quad (2)$$

which implies that

$$\sum_i A_i^2 \approx \sum_\alpha n_\alpha \mathcal{A}_\alpha^2 \sum_u |\Psi(\mathbf{r}_u)|^4 = \sum_\alpha \frac{n_\alpha \mathcal{A}_\alpha^2}{N}, \quad (3)$$

where  $n_\alpha$  is the average number of nuclei of this species in the unit cell (i.e. in III-V compounds we have  $\sum_\alpha n_\alpha = 2$ ), and the sum over  $u$  is over all the Wigner-Seitz unit cells.

The hf Hamiltonian can be written as  $\hat{H}_{\text{hf}} = \hat{\mathbf{S}} \cdot \hat{\mathbf{h}}$ , where we have introduced the *Overhauser field* operator  $\hat{\mathbf{h}} = \sum_i A_i \hat{\mathbf{J}}_i$ . In some cases (discussed below) one can neglect the quantum dynamics of  $\hat{\mathbf{h}}(t)$  (written here in Heisenberg picture), and replace it by classical vector  $\mathbf{h}$ . The quantum averages measured in a given experimental setup are then replaced by classical averages over an appropriate distribution of  $\mathbf{h}$ . In this picture we see that the loss of coherence of the electron spin is due to an averaging over electron precession about randomly distributed effective magnetic fields  $\mathbf{h}$ .

Another representation of the hf Hamiltonian which will prove useful in the following discussion is

$$\hat{H}_{\text{hf}} = \hat{h}^z \hat{S}^z + \hat{V}_{\text{ff}}, \quad (4)$$

where

$$\hat{V}_{\text{ff}} = \hat{h}^x \hat{S}^x + \hat{h}^y \hat{S}^y = \frac{1}{2}(\hat{h}^+ \hat{S}^- + \hat{h}^- \hat{S}^+), \quad (5)$$

is the electron-nuclear flip-flop operator. Note that in this flip-flop term we find the transverse (with respect to the magnetic field defining the  $z$  axis) components of the Overhauser field,  $h_\perp$ .

The Hamiltonian in Eq. (1) is very often called *the central spin Hamiltonian*.<sup>2</sup> This Hamiltonian is in fact integrable, and it can be diagonalized with the help of Bethe ansatz, as was first done by Gaudin [26]. However, it has to be stressed that the integrability of the problem does not allow for obtaining the solution for *dynamics* of a system with an appreciable number  $N$  of spins, since for the calculation of central spin coherence dynamics one needs the full spectrum of the Hamiltonian with the corresponding eigenstates. The brute-force numerical treatment of the problem requires dealing with a Hilbert space of dimension  $2^N$ , while in Gaudin solution one only needs to deal with  $\sim N$  degrees of freedom - but one has to solve a set of  $\sim N$  nonlinear coupled Bethe equations for these quantities. It turns out that this task is manageable only for  $N \leq 20$  (see [27] and [28]), which is in fact the same as the system size which can be treated with appropriate numerical methods for quantum state evolution [29]. Gaudin's solution is also impossible in the case of all nuclei not having the same Zeeman splitting - a situation which exists for III-V quantum dots, and which is very important for theory of spin echo decay in this system [H2,H3].

The Hamiltonian of the whole system (the qubit and the bath) contains also the qubit's part:

$$H_Q = \Omega \hat{S}^z + \hat{H}_{\text{control}}(t) \quad (6)$$

---

<sup>2</sup>It should be noted that the term "central spin problem" is often used to refer to any system in which we have the "central" spin of interest (the qubit) which is coupled to many other spins comprising the bath. The qubit-bath coupling does not have to be of the Heisenberg form, and the self-Hamiltonian of the bath can have many forms. The Hamiltonian of the electron interacting with the nuclear spins in a quantum dot described here belongs to such a generalized class of central spin problems when the dipolar interaction between the nuclear spins is included.

where  $\Omega$  is the Zeeman splitting, and  $\hat{H}_{\text{control}}(t)$  represents the time-dependent external control fields. Here I will only consider external controls in the form of very short pulses performing rotations of the qubit's state, say  $\pi$  or  $\pi/2$  rotations about the  $x$  axis.

The final element of the microscopic description of the system is the Hamiltonian of the bath itself:

$$\hat{H}_{\text{bath}} = \sum_i \omega_{\alpha[i]} \hat{J}_i^z + \hat{H}_{\text{dip}} , \quad (7)$$

where  $\omega_{\alpha}$  is the Zeeman splitting of the nucleus of the  $\alpha$  species, and  $\hat{H}_{\text{dip}}$  is the Hamiltonian of the dipolar interactions between the nuclear spins. For magnetic fields used in almost all the experiments on spin qubits these interactions can be assumed to conserve the net  $z$  component of the nuclear spin:

$$\hat{H}_{\text{dip}} = \sum_{i \neq j} b_{ij} (\hat{J}_i^+ \hat{J}_j^- - 2\hat{J}_i^z \hat{J}_j^z) , \quad (8)$$

where the summation is over the nuclei  $i$  and  $j$  of the same species, and the couplings are given by

$$b_{ij} = -\frac{1}{2} \hbar \gamma_i \gamma_j \frac{1 - 3 \cos^2 \theta_{ij}}{r_{ij}^3} \quad (9)$$

where  $r_{ij}$  is the distance between the two nuclei and  $\theta_{ij}$  is the angle of  $\mathbf{r}_{ij}$  relative to the  $B$  field direction.

### ***Energy scales in the Hamiltonian and their basic consequences***

It is crucial to note the smallness of the energy scale of the intrinsic Hamiltonian of the bath compared to the typical temperatures at which the experiments are conducted. For  $B$  fields used in experiments (which rarely exceed one Tesla, and are always less than about 10 Teslas) the nuclear Zeeman energies  $\omega_{\alpha}$  are of the order of  $0.1 \mu\text{eV}$ , which corresponds to about  $0.1 \text{ mK}$ . Furthermore, the nearest-neighbour dipolar couplings are of the order of  $0.1 \text{ peV}$ , which corresponds to  $\sim 1 \text{ nK}$ . This means that even in the best dilution fridges, reaching temperatures  $\sim 1 \text{ mK}$ , the thermal equilibrium density matrix of the nuclei will be  $\hat{\rho}_J \sim \mathbb{1}$ . The other consequence is the slowness of the intrinsic nuclear dynamics. In fact, it is not obvious that in a given experiment the average over many repetitions of the cycle of qubit initialization-evolution-measurement is equivalent to averaging over this density matrix, *i.e.* that the time averaging is equivalent to ensemble averaging. In other words, the ergodicity of the nuclear dynamics should not be taken for granted when considering real experimental situations.

Let us look more closely at intrinsic nuclear dynamics. The transverse components of the Overhauser field,  $h_{\perp}$ , decorrelate on timescale of  $\tau_{\perp} \sim 100 \mu\text{s}$  in III-V materials, which is set by the broadening of the nuclear resonance lines by dipolar interactions [*i.e.* the spread of nuclear energy splittings due to the  $\sum_{i,j} b_{ij} \hat{J}_i^z \hat{J}_j^z$  term in Eq. (8)]. At finite  $B$  field we also have Larmor precession of  $h^{x,y}$ , and in the range of  $B$  relevant for experiments on III-V QDs the period of this precession is much shorter than  $\tau_{\perp}$ . Such a coherent precession of a macroscopic number of nuclear spins has a striking impact on the dynamics of spin echo decay, see Section 4.2.4. On the other hand, the longitudinal component of the Overhauser field,  $h^z$ , decorrelates on a much longer timescale  $\tau_{\parallel}$ .  $h^z$  changes due to nearest-neighbour flip-flops [the first term in Eq. (8)], and the cumulative effect of many such flip-flops can be described as a process of nuclear *spin diffusion* [30]. Given the nuclear spin diffusion constant  $D$  and the size  $L$  of the QD, we have  $\tau_{\parallel} \sim L^2/D$ , which is  $\sim 1 - 10$  minutes in gated quantum dots.<sup>3</sup> The experiments give the decorrelation time of  $\sim 10 \text{ s}$  in GaAs [32], in qualitative agreement with theory [33].

---

<sup>3</sup>The thing to note is that the gated dots are strain-free relatively to the self-assembled ones. In the latter, the spatially inhomogeneous strain leads to local gradient of electric fields, and thus to quadrupolar splittings of the nuclei. These splittings can strongly suppress the nuclear spin diffusion, and the longitudinal Overhauser field dynamics in SAQDs can be even slower, with nuclear polarization in these QDs persisting for at least tens of minutes [31].

In the presence of the electron the  $k$ -th nucleus experiences the Knight field  $\sim A_k$ , the maximum value of which is  $\sim \mathcal{A}/N$  (for simplicity I use here the fact that in III-V materials all  $\mathcal{A}_\alpha$  are of the same order of magnitude). This quantity, which in GaAs QD with  $N \sim 10^6$  is  $\sim 0.1$  neV, is also the spread of  $A_k$  couplings. From time-energy uncertainty principle we can expect that for times much shorter than  $N/\mathcal{A} \sim 10 \mu\text{s}$ , the inhomogeneity of the couplings should not have any impact on system's dynamics, while at much longer times the exact distribution of  $A_k$  (i.e. the shape of the electron's wavefunction) could matter. This observation will be important for many of the following considerations.

The last important observation is related to the mismatch of electronic and nuclear Zeeman splittings:  $\Omega \approx 1000 \cdot \omega_\alpha$  due to the ratio of electronic and nuclear magnetons. We focus here on magnetic field for which  $\Omega$  is much larger than the Overhauser field felt by the electron<sup>4</sup> (which is  $\sim 1$  mT in GaAs, see below), and  $\omega_\alpha$  is much larger than the dipolar broadening of nuclear spin splittings (which corresponds to a field of about 0.1 mT). At such fields  $\Omega \gg \omega_\alpha$  means that the direct electron-nuclear flip-flop described by Eq. (5) is energetically forbidden. It is thus natural to treat the  $\hat{V}_{\text{ff}}$  term perturbatively, as it only leads to *virtual* transitions, which in the second order of perturbation theory lead to appearance of effective electron-mediated interactions between the nuclei. An equivalent statement is that at large  $B$  the influence of  $h_\perp$  field is strongly suppressed, with this field contributing a correction to spin splitting  $\sim h_\perp^2/\Omega$  and giving a small tilt of the quantization axis away from the  $z$  direction by angle  $\sim h_\perp/\Omega$ .

Taking all the above into account we can safely assume that on timescales of less than a few  $\mu\text{s}$  the nuclear bath is static, and then we can replace tracing over the nuclear density matrix by averaging over a classical distribution of static Overhauser fields. Since the number of nuclei  $N$  is large, the distribution of these fields (applicable when the signal averaging time is longer than the autocorrelation time of  $h^z$ ) is Gaussian [22–24]:

$$P(\mathbf{h}) = \frac{1}{(2\pi)^{3/2}\sigma^3} \exp\left(-\frac{h^2}{2\sigma^2}\right), \quad (10)$$

with

$$\sigma^2 = \frac{1}{3} \sum_\alpha J_\alpha(J_\alpha + 1) \sum_{i \in \alpha} A_i^2 = \frac{1}{3} \sum_\alpha J_\alpha(J_\alpha + 1) n_\alpha \frac{\mathcal{A}_\alpha^2}{N}. \quad (11)$$

The standard deviation  $\sigma$  of the distribution of the Overhauser field is an important quantity: this is the typical value of the effective field exerted by the nuclei on the electron. In gated dots made of GaAs,  $\sigma$  corresponds to a field of about 3 mT.

#### 4.2.2 Electron spin decoherence due to its interaction with the nuclear bath: basic considerations

When  $\Omega \gg \sigma$  we can either completely neglect the influence of  $h_\perp$  (or equivalently  $\hat{V}_{\text{ff}}$ ), or perturbatively replace it by an effective electron-mediated inter-nuclear interaction. The latter case will be discussed in detail in Section 4.2.4. Here we only focus on the fact that in both situations we will deal with *pure dephasing* Hamiltonian:

$$\hat{H} = \Omega \hat{S}^z + \hat{H}_B + \hat{S}^z \hat{V}, \quad (12)$$

where  $\hat{H}_B$  is the bath Hamiltonian, and  $\hat{V}$  is the bath operator coupling to the  $z$  component of the electron spin. With such a Hamiltonian, the diagonal elements of the reduced density matrix of the qubit are constant, and interaction with the environment causes only the decay of the off-diagonal element,

$$\rho_{+-}^S(t) \equiv \langle + | \text{Tr}_J \hat{\rho}(t) | - \rangle \langle + | \text{Tr}_J e^{-i\hat{H}t} \hat{\rho}(0) e^{i\hat{H}t} | - \rangle, \quad (13)$$

---

<sup>4</sup>This corresponds to a very reasonable, from the point of view of qubit control, requirement that the electron spin splitting and the direction of its quantization axis is mostly due to the external  $B$ , with nuclei giving only a small correction.

in which  $|\pm\rangle$  are eigenstates of  $\hat{S}^z$ ,  $\hat{\rho}(t)$  is the density matrix of the total system, and  $\text{Tr}_J$  is the partial trace over the nuclear degrees of freedom. Let us define the *decoherence function*  $W(t)$ , which for the case of free evolution of the spin is given by

$$W_{\text{FID}}(t) = \frac{\rho_{+-}^S(t)}{\rho_{+-}^S(0)} = \langle e^{i\hat{H}_-t} e^{-i\hat{H}_+t} \rangle, \quad (14)$$

where  $\langle \dots \rangle \equiv \text{Tr}_J [\hat{\rho}_J(0) \dots]$ , and

$$\hat{H}_{\pm} = \pm\Omega/2 + \hat{H}_B \pm \hat{V}/2. \quad (15)$$

The calculation of qubit's dephasing is now mapped on averaging (over the initial density matrix of the bath) of a specific evolution of the bath itself: equation (14) can be interpreted as an average of the evolution due to  $\hat{H}_+$  forward in time, followed by backward-in-time evolution under  $\hat{H}_-$ . This can be viewed as a variation of a typical structure encountered in nonequilibrium quantum statistical mechanics [34], an average over an evolution defined on a closed time-loop contour. This structure allows for use of methods of diagrammatic perturbation theory, as we will see in Section 4.2.4.

### *Inhomogeneously broadened free induction decay*

In most of the experiments on single QDs, the total time of data acquisition (a cycle of qubit initialization-evolution-readout repeated many times) is longer than a minute. This means that the result of the experiment corresponds to averaging of the qubit's evolution over the equilibrium nuclear density matrix. The same situation is of course encountered in experiments on ensembles of optically-excited self-assembled quantum dots [35, 36]. The measured dephasing of the electron is then dominated by the ensemble averaging, and it occurs on timescale on which the bath dynamics is irrelevant.

As already mentioned, for  $\Omega \gg \sigma$  the effects of  $h_{\perp}$  are suppressed. On the other hand, the averaging over the  $h^z$  component leads to very strong dephasing of the electron spin. Let us focus on standard free evolution experiment (called "free induction decay", FID, in most of literature, in deference to old terminology of NMR), in which the electron spin is initialized in the  $xy$  plane, it is allowed to freely precess for time  $t$ , and finally it is rotated again to the  $z$  axis and subjected to a projective measurement. From many repetitions of such an experiment (with many measurements taken for each delay  $t$ ) the time-dependence of  $\langle \hat{S}^{x,y}(t) \rangle$  is obtained. The expected result is the average of precession over a Gaussian distribution of precession frequencies,  $\Omega + h^z$ , which reads

$$\langle \hat{S}^x(t) \rangle = \frac{1}{2} \cos(\Omega t) e^{-(t/T_2^*)^2}, \quad (16)$$

where the inhomogeneous broadening dephasing time  $T_2^* = \sqrt{2}/\sigma$  [with  $\sigma$  given by Eq. (11)] is about 10 ns in GaAs QDs, which is much shorter than the timescales of nuclear dynamics discussed in the previous section. We can see that in this case the quasi-static bath approximation (QSBA), in which the nuclei are treated as static during each instance of spin evolution, but their fluctuations due to their dynamics *between* the repetitions of the experiment are taken into account, is justified. Such a fast Gaussian decay of spin coherence was confirmed in many experiments [6, 37–40]

However, in the context of quantum computation, the dephasing due to inhomogeneous broadening is not the fundamental obstacle. The  $T_2^*$  decay comes from inefficient and noisy readout process enforcing very long data acquisition time. The apparent dephasing is only due to our lack of knowledge about the initial value of  $h^z$  - if this value was known at the beginning of the experiment, then, provided that the experiment took less than a few minutes, there would be much less averaging over  $h^z$  involved. In fact, single-shot readout schemes (which are most probably necessary anyway for operation of any realistic quantum computation circuit) were developed for quantum dots [41], allowing for shortening of the experiment duration by orders of

magnitude, down to times significantly shorter than the  $h^z$  autocorrelation time. Furthermore, if we are interested in using the qubit as a quantum memory, the effects of quasi-static energy shifts of the qubit can be removed by the application of the spin echo pulse sequence [30, 42]. Let us now review these methods of “looking beneath the inhomogenous broadening”.

### *Spin echo and its generalizations*

In a spin echo (SE) experiment the spin initialization and readout are the same as in FID, but the spin is additionally rotated by angle  $\pi$  around one of the in-plane axes at the midpoint of its evolution, at time  $t/2$ . Such a pulse sequences can be written as  $t/2 - \pi - t/2$ . This procedure will remove the static (on timescale of  $t$ ) spread of the precession frequencies, since the evolution of every spin during the first period of  $t/2$  will be undone during the second  $t/2$  period after the pulse. This refocusing of the spins of course does not work perfectly when the bath is dynamic, so the amplitude of the SE signal will decay with increasing  $t$ .

The multi-pulse generalizations of SE have been used in NMR for more than 60 years now [43], with the simplest example being the Carr-Purcell sequence,<sup>5</sup> which can be written as  $t/2n - \pi - t/n - \pi - \dots - \pi - t/n - \pi - t/2n$ , with  $n$  being the number of pulses. In the modern context of protection of coherence of individual qubits, the multi-pulse echo-like procedures come under the name of *dynamical decoupling* (DD) [44–46] (*i.e.* decoupling of the qubit from its environment by driving it). Due to potential importance of various DD sequences for long-lasting protection of qubit’s coherence, it is important for a theory of decoherence to easily take into account various spacings of many pulses. The theory presented in Section 4.2.4 has this useful feature.

The evolution of  $\rho_{+-}^S$  in the case of SE (and for  $\pi_x$  pulse) is given by

$$\rho_{+-}^S(t) = \text{Tr}_J \langle + | e^{-i\hat{H}t/2} (-i\hat{\sigma}_x) e^{-i\hat{H}t/2} \hat{\rho}_J(0) \hat{\rho}^S(0) e^{i\hat{H}t/2} (i\hat{\sigma}_x) e^{i\hat{H}t/2} | - \rangle , \quad (17)$$

which for the pure dephasing case is equal to

$$\rho_{+-}^S(t) = \rho_{-+}^S(0) W_{\text{SE}}(t) = \rho_{-+}^S(0) \left\langle e^{i\hat{H}_+t/2} e^{i\hat{H}_-t/2} e^{-i\hat{H}_+t/2} e^{-i\hat{H}_-t/2} \right\rangle , \quad (18)$$

where the decoherence function for the SE case,  $W_{\text{SE}}(t)$ , is defined. The decoherence functions for DD sequences with more pulses are defined in an analogous way.

### *Narrowed state free induction decay*

While the echo experiments have been routinely performed in NMR and ESR for past 60 years, the idea of narrowing of the state of the nuclear bath is much younger [47–49], since it pertains to measurements on a *single* spin, and only during the last 10 years it has become experimentally possible to address individual spins. The idea is to pre-measure the value of  $h^z$  before the FID experiment is done. Of course this makes sense when we can assume that this  $h^z$  does not change during the gathering of data. In fact, the most natural way of measuring the narrowed state free induction decay (NFID) is to perform the whole experiment during time much shorter than  $h^z$  decorrelation time. This was done in gated quantum dots by using a sensitive setup for single-shot readout of spin states [50]. When the datapoints for various time delays between the initialization and readout are all taken during only about 100 ms, the FID signal *does not* exhibit the  $T_2^*$  decay. Instead, spin precession with frequency given by  $\Omega + h^z$  was seen, and there was practically no decay of the oscillation amplitude visible for time delay of less than a microsecond.<sup>6</sup>

<sup>5</sup>Experimentally the modification of this sequence introduced by Meiboom and Gill is usually implemented. The difference in CP and CPMG sequences is the choice of in-plane axes about which the rotations are performed, with the CPMG choice leading to results more robust to systematic pulse errors. This is irrelevant here, since I consider ideal  $\pi$  and  $\pi/2$  pulses.

<sup>6</sup>There are many other experiments showing various degrees of narrowing of nuclear field distributions in both gated QDs (e.g. [9]) and in ensembles of self-assembled QDs [31, 35], but the example given above seems to me to be the nicest illustration of the separation of timescales specific to the nuclear bath.

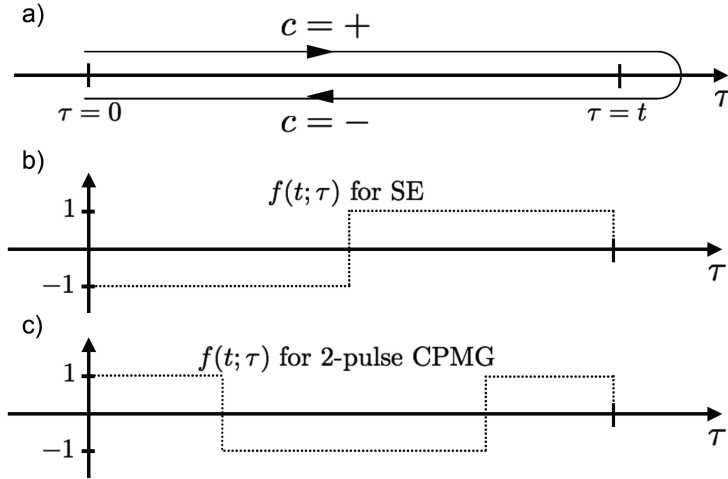


Figure 1: a) The closed loop contour along which the operators in Eq. (19) are ordered. b) The plot of the time-domain filter function  $f(t; \tau) \equiv f_t(\tau)$  for the Spin Echo sequence. c) The same for 2-pulse CPMG sequence. The Figure is adapted from Ref. [H3].

In order to theoretically model the “ideal” NFID experiment, one has to calculate the evolution of the electron spin using Eq. (14), but assuming an initial nuclear density matrix  $\hat{\rho}^J(0)$  describing the state with a well-defined value of  $h^z$ .

#### *Causes of decoherence in SE and NFID experiments*

In these experiments the quasi-static fluctuations of  $h^z$  are irrelevant: in SE they are cancelled by the pulse sequence, in NFID the value of  $h^z$  at the beginning of electron precession is pre-measured. The decay of coherence in these cases is then caused by two mechanisms:

1. Dynamics of  $\hat{h}^z$  occurring on timescale of electron spin evolution.
2. The residual coupling of the electron spin to  $h_{\perp}$ . Here, depending on timescale of interest, both the quasi-static case (averaging over static  $h^x$  and  $h^y$  fields) and the dynamical case (involving the actual fluctuations of nuclear spins due to the  $\hat{V}_{\text{ff}}$  term) need to be considered.

The first mechanism will be briefly outlined in Section 4.2.3. The second mechanism will be explained in more detail in Section 4.2.4.

#### **4.2.3 Spin decoherence at very high magnetic fields: cluster expansion theory for dipolar dynamics of the nuclear bath**

For high enough<sup>7</sup> magnetic field the  $\hat{V}_{\text{ff}}$  operator in Eq. (1) can be completely neglected, and the only qubit-bath coupling remaining is  $S^z \hat{h}^z$ . The  $h^z$  field fluctuates then due to the presence of inter-nuclear flip-flop terms in the Hamiltonian of the dipolar interaction, Eq. (8). Note that under this approximation  $\Omega$  simply disappears from the calculation of spin coherence: the theory outlined in this section gives results independent of  $\Omega$ .

All the above formulas for  $W(t)$  can then be rewritten as

$$W(t) = \left\langle \mathcal{T}_c \exp \left( -i \int_c \hat{\mathcal{H}}_{\text{dip}}(\tau_c) d\tau_c \right) \right\rangle, \quad (19)$$

<sup>7</sup>The precise meaning of what I mean by “high enough” will be explained in Section 4.2.4, where the theory taking  $\hat{V}_{\text{ff}}$  into account will be given.

where  $\mathcal{T}_c$  denotes ordering of the operators on the contour shown in Fig. 1a,  $\tau_c = (\tau, c)$  with  $\tau$  being the time variable and  $c = \pm$  being the contour branch label, and  $\hat{\mathcal{H}}_{\text{dip}}(\tau_c)$  is the dipolar interaction written in an interaction picture on a contour. The nuclear operators within  $\hat{\mathcal{H}}_{\text{dip}}(\tau_c)$  are given by

$$\hat{J}_k^\pm(\tau_c) = \hat{J}_k^\pm \exp \left[ \pm i\omega_k \tau \pm ic \int_0^\tau f_t(t') \frac{A_k}{2} dt' \right], \quad (20)$$

where the slightly nonstandard second term in the exponent comes from the fact that we have introduced an interaction picture with respect to a time-dependent operator

$$\hat{H}_0^\pm(\tau_c) = \sum_k \omega_k \hat{J}_k^z + cf_t(\tau) \hat{h}^z / 2. \quad (21)$$

in which  $f_t(\tau)$  is the temporal filter function specific to the pulse sequence (see Fig. 1b and 1c for examples).

The theoretical task is now reduced to performing a quantum average of a generalized exponent in Eq. (19). A natural approach to such a problem is the linked cluster expansion, in which the average of the exponent is rewritten as an exponent of a sum of linked (in diagrammatic sense) terms in the expansion of  $W(t)$ . Note that in any diagrammatic representation of perturbation series the disconnectedness of a given diagram is equivalent to statistical independence of the disconnected contributions. From this point of view it should be clear that the diagrammatic linked cluster expansion is closely related to the cumulant expansion [51].

The difficulty with this approach is caused to the fact that spins have neither fermionic nor bosonic statistics, and the standard methods of many-body diagrammatic perturbation theory *do not apply here*. Rather cumbersome adaptations of diagrammatic methods and Feynman rules to the spin bath problem have to be used [52, 53], and the calculation of linked clusters becomes very complicated beyond the second order in  $\hat{H}_{\text{dip}}$ . This technical problem was circumvented by development of cluster expansion methods in which one had to simply numerically obtain the evolution of an electron coupled to given real-space cluster of nuclei and use these calculations to construct a solution corresponding to a certain resummation of the diagrammatic linked cluster expansion [53, 54]. These calculations showed that the SE and NFID decay due to dipolar nuclear dynamics can be well-described<sup>8</sup> by simply taking the two-spin clusters [54–57], while the use of multi-pulse DD sequences might necessitate the calculation of dynamics due to larger clusters [58, 59]. The physical explanation of this result is simple: on the timescale  $T_2$  defined by  $W(T_2) = 1/e$  the non-trivial correlations among groups of more than two nuclear spins are not built-up yet, and irreducible dynamics of only pairs of spins in the bath has to be taken into account. Let me note that this theory [52, 54–56] has been very succesful at explaining the SE results obtained for electron spins bound to phosphorous donors in silicon [60, 61].

#### 4.2.4 Theory of spin qubit decoherence caused by interaction with the nuclear bath at low magnetic fields

The theory of dephasing due to dipolar induced dynamics of nuclei outlined in the previous section predicts  $W = \exp[-(t/T_2)^4]$  in GaAs QDs for both SE and NFID, with  $T_2 \sim 10 - 50 \mu\text{s}$  (depending on the QD shape) [54, 56, 57]. This prediction was in very visible disagreement with the experimental SE results available in 2008 [6, 7]. This simply meant that the  $B$  fields used in these experiments were not “high enough”, but the theory dealing with smaller  $B$  fields was lacking. The papers [H2,H3] were written in response to this challenge.

##### *Effective Hamiltonian and ring diagram theory*

The starting point is the effective Hamiltonian  $\hat{H}$  of hf-mediated interactions [56, 62] obtained

---

<sup>8</sup>By “well-described” I mean that the theory correctly captures the characteristic decay time  $T_2$  and the time-dependence of  $W(t)$  for  $t$  comparable to this  $T_2$ , and possibly somewhat larger.

from the full hf Hamiltonian by a canonical transformation:  $\tilde{H} = e^{\hat{S}} \hat{H} e^{\hat{S}}$ , where  $\hat{S}$  is an anti-Hermitian operator chosen to remove  $\hat{V}_{\text{ff}}$  from  $\hat{H}$ . In order to obtain the lowest-order (in  $\hat{V}_{\text{ff}}$ ) expression for  $\tilde{H}$  we use  $\hat{S} = \frac{2}{\Omega} \hat{V}_{\text{ff}} \hat{S}^z$ , and expanding  $\tilde{H}$  we obtain

$$\tilde{H}^{(2)} = \hat{S}^z \sum_{i,j} \frac{A_i A_j}{4\Omega} (\hat{J}_i^+ \hat{J}_j^- + \hat{J}_i^- \hat{J}_j^+) . \quad (22)$$

It should be noted that the transformation of states,  $|\tilde{\psi}\rangle = e^{-\hat{S}} |\psi\rangle$ , which in principle should accompany the transformation of the Hamiltonian, is neglected here. Although this is a rather standard step, and approximate justifications for taking it were given [56], the influence of this approximation on calculations of spin decoherence remains somewhat controversial (see Section 4.2.7 for more discussion). However, we will soon see that this approximation has been highly successful at predicting SE signal decay, and for now we close this discussion with such an empirical argument.

The above transformation can lead to a reasonable approximation only when  $\Omega \gg \sigma$ , i.e. the small parameter controlling the applicability of the effective Hamiltonian is

$$\delta \equiv \frac{\sigma}{\Omega} . \quad (23)$$

This is clear from a classical reasoning. In the presence of  $\mathbf{h}$  field the qubit's quantization axis and its splitting is perturbed. If we disregard the tilting of the axis (which is roughly equivalent to disregarding the transformation of states above), we only have to deal with the influence of  $\mathbf{h}$  on splitting, which is given by

$$\tilde{\Omega} = \sqrt{(\Omega + h_z)^2 + h_{\perp}^2} \approx \Omega + h_z + \frac{h_{\perp}^2}{2\Omega} , \quad (24)$$

where  $\Omega \gg \sigma$  is assumed (with  $\sigma$  being the estimate of the maximal value of  $h_{\perp}$ ). It is easy to check that Eq. (22) is simply the quantum version of the  $h_{\perp}^2/2\Omega$  term appearing above.

We write now the decoherence function analogous to the one from Eq. (19)

$$W(t) = \left\langle \mathcal{T}_C \exp \left( -i \int_C c f_t(\tau) \tilde{\mathcal{V}}(\tau_c) d\tau_c \right) \right\rangle , \quad (25)$$

where  $\tilde{\mathcal{V}}$  is 1/2 times  $\tilde{H}^{(2)}$  written in the interaction picture defined in Eq. (20). Note the additional presence of the contour index  $c = \pm$  and the filter function  $f_t(\tau)$  in the exponent: this is due to the fact that the hf-mediated interaction is conditioned on  $S^z$ .

Taking only the lowest-order terms in linked cluster expansion (as it can be done for dipolar interactions within the bath, see Section 4.2.3) is not a good approximation now, because the interaction from Eq. (22) is coupling *all* the  $N$  spins. However, the long-range nature of the interaction allows for a different kind of solution. Expanding Eq. (25) we encounter averages of products of many  $J_k^{\pm}$  operators. For both the thermal and the narrowed nuclear density matrix, each  $J_k^+$  has to be paired with  $J_k^-$  in order for the average to be non-vanishing. Most importantly, since every spin is coupled with similar strength to every other of  $\sim N$  spins, in  $k$ -th order of expansion there are  $\sim N^k$  terms with a *maximal* number of *distinct* nuclear indices. These are the *ring diagrams*, the leading order terms in  $1/N$  expansion<sup>9</sup> of averages appearing in calculation of Eq. (25). They are easy to evaluate, because taking the leading order terms in  $1/N$  expansion means that the nuclear spins involved in different pairings are distinct, and as a consequence the spin operators can be assumed to commute inside the averaging bracket:  $\langle [J_k^+, J_l^-] \rangle = 2pJ\delta_{kl}$ , where  $p$  is the average polarization of the nuclear spins. In the case of  $p=0$

<sup>9</sup>Note the close relation between this solution to the calculations of partition function of long-range Ising model [63]. The difference in the quantum case at hand is that we have to deal with a generalized contour-ordered exponent.

$$\begin{aligned}
\text{a) } W^{(2)} &= -\frac{1}{2} \times \text{circle with two dots} = -\frac{1}{2} \sum_{k \neq l} T_{kl} T_{lk} \\
\text{b) } W^{(3)} &= \frac{(-i)^3}{3!} \times 2 \times \text{triangle} = \frac{i}{3} \sum_{k \neq l \neq m} T_{kl} T_{lm} T_{mk} \\
\text{c) } W^{(4)} &\approx \frac{(-i)^4}{4!} \left( 6 \times \text{square} + 3 \times \text{circle} \times \text{circle} \right) \\
\text{d) } W &\approx \exp \left( \frac{(-i)^2}{2} \text{circle with two dots} + \frac{(-i)^3}{3} \text{triangle} + \frac{(-i)^4}{4} \text{square} + \dots \right)
\end{aligned}$$

Figure 2: Graphical representations of lowest-order ring diagrams appearing in the expansion of  $W(t)$  and the exponential resummation of these terms. The Figure is adapted from Ref. [H3].

considered in [H2-H4] this simply means that the spin operators effectively commute, i.e. when calculating the ring diagrams we can use Wick's theorem. Furthermore, a ring diagram appearing in the  $k$ -th order of expansion,  $R_k$ , is a linked one, and combinatorics of pairings (see Fig. 2) leads us to

$$W(t) \approx \exp \left( \sum_{k=1}^{\infty} \frac{(-i)^k}{k} R_k(t) \right). \quad (26)$$

The expressions for  $R_k$  have a cyclical structure (which justifies the name given to such a term) allowing us to write

$$R_k = \sum_{i_1 \neq i_2 \neq \dots \neq i_k} T_{i_1 i_2}(t) \dots T_{i_k i_1}(t) \approx \text{Tr}[\mathbf{T}(t)]^k, \quad (27)$$

where  $T_{kl}$  is the  $T$ -matrix given by

$$T_{kl}(t) = \sqrt{\langle J_k^+ J_k^- \rangle \langle J_l^+ J_l^- \rangle} \int_{\mathcal{C}} cf(t; \tau) \tilde{\mathcal{V}}(\tau_c) d\tau_c. \quad (28)$$

The calculation of decoherence requires then diagonalization of  $N \times N$  matrix. However, in practice we can simplify the problem even more. Instead of dealing with the full  $T$ -matrix, we can use an effective coarse-grained  $\tilde{T}$ -matrix, which appears when we write Eq. (27) in the continuum limit, replacing the sums over the nuclei by integrals over appropriate density  $\rho(A)$  of hf couplings, and then replace  $\rho(A)$  by an approximate piecewise-constant function. This corresponds to replacing the real envelope wavefunction  $\Psi(\mathbf{r})$  by a “wedding cake” function. It is easy to check then what number of coarse-graining steps,  $M$ , is needed to obtain a good approximation for  $W(t)$  on a given timescale. For example, for  $t \ll N/\mathcal{A}$ , we can use  $M=1$ , and for a bath with  $N_J$  nuclear species ( $N_J=3$  for GaAs) it is enough to use a  $\tilde{T}$ -matrix of dimension  $N_J \times N_J$ .

### **Results for narrowed state free induction decay (NFID)**

In the case of NFID the  $T$ -matrix is particularly simple at short times  $t \ll 1/(A_k - A_l), 1/(\omega_k - \omega_l)$ :

$$T_{kl} \approx \langle J_\alpha^+ J_\alpha^- \rangle \frac{A_k A_l}{2\Omega} t, \quad (29)$$

from which we get that

$$R_k(t) = \sum_{\alpha} \left( \frac{n_{\alpha} \frac{1}{3} J_{\alpha} (J_{\alpha} + 1) \mathcal{A}_{\alpha}^2 t}{N\Omega} \right)^k \equiv (\eta t)^k, \quad (30)$$

where we have used the fact that in an unpolarized bath  $\langle J_{\alpha}^+ J_{\alpha}^- \rangle = \frac{2}{3} J_{\alpha} (J_{\alpha} + 1)$ . We can now write out all the terms appearing in the exponent in Eq. (26). Then we have to note that the

obtained power series' define functions that can be analytically continued to any values of  $t$ . In this way we obtain

$$W_{NFID}(t) = e^{-i(\Omega+h_z)t} \frac{e^{-i \arctan \eta t}}{\sqrt{1 + \eta^2 t^2}}. \quad (31)$$

This result can also be obtained using a classical calculation involving averaging over a quasi-static distribution of  $h_\perp$  fields [H5]. We take the expression for qubit splitting from Eq. (24) and we obtain

$$\langle e^{-i\tilde{\Omega}t} \rangle = e^{-i(\Omega+h_z)t} \int \frac{1}{2\pi\sigma^2} e^{-h_\perp^2/2\sigma^2} e^{-ith_\perp^2/2\Omega} d^2h_\perp = e^{-i(\Omega+h_z)t} \frac{1}{1 + it\frac{\sigma^2}{\Omega}}, \quad (32)$$

which is in fact equal to Eq. (31) once we plug in the values of  $\sigma^2$  from Eq. (11), giving us  $\eta = \sigma^2/\Omega$ , and we notice that  $\cos \arctan \eta t = 1/\sqrt{1 + \eta^2 t^2}$  and  $\sin \arctan \eta t = \eta t/\sqrt{1 + \eta^2 t^2}$ . This is an example of how performing the resummation of all the ring diagrams is a generalization of performing Gaussian average over phase which is proportional to a square of the random variable. We will encounter the same structure in Section 4.3.2.

At long times,  $t \gg N/\mathcal{A}$ , we have a very different solution. We obtain then the following expression for  $R_k^\alpha$  due to nuclei of species  $\alpha$ :

$$R_k^\alpha = n_\alpha^k a_\alpha^k \int dA_1 \dots \int dA_k \rho_\alpha(A_1) \dots \rho_\alpha(A_k) \frac{A_1^2 \dots A_k^2}{(2\Omega)^2} \frac{\sin A_{12}t}{A_{12}} \frac{\sin A_{23}t}{A_{23}} \dots \frac{\sin A_{k1}t}{A_{k1}} \quad (33)$$

where  $A_{kl} = (A_k - A_l)/2$ ,  $a_\alpha \equiv \frac{2}{3} J_\alpha (J_\alpha + 1)$  and the density of  $A_k$  couplings,  $\rho(A)$ , is

$$\rho_\alpha(A) = \frac{1}{\nu_0} \int_V \delta[A - \mathcal{A}_\alpha |\Psi(\mathbf{r})|^2] d^3r. \quad (34)$$

In [H2,H3] it was discussed, based on numerical results of diagonalization of coarse-grained  $\tilde{T}$ -matrices, how in the  $\mathcal{A}/\Omega \ll 1$  limit (i.e. when  $B \gg$  a few Tesla in GaAs) the  $R_2$  term dominates the sum over all the rings.<sup>10</sup> Using the fact that for  $A_{kl}t \rightarrow \infty$  we have  $\text{sinc}^2 A_{kl}t \rightarrow \frac{\pi}{t} \delta(A_{kl})$  we arrive at

$$R_2^\alpha \approx t \frac{\pi a_\alpha^2 n_\alpha^2}{2\Omega^2} \int \rho_\alpha^2(A) A^4 dA \equiv \frac{2t}{T_{2,\text{long}}^\alpha}, \quad (35)$$

and the result for coherence decay at high  $B$  fields (for which this decay indeed occurs at long times)

$$W_{NFID}(t \gg N/\mathcal{A}) \approx \exp\left(-\frac{t}{T_{2,\text{long}}}\right), \quad (36)$$

with  $T_{2,\text{long}}^{-1} = \sum_\alpha (T_{2,\text{long}}^\alpha)^{-1}$ . Note that  $T_{2,\text{long}} \sim N\Omega^2/\mathcal{A}^3$ , so that the characteristic decay time in this regime is longer by a factor of  $\Omega/\mathcal{A}$  than the half-decay time ( $\sim 1/\eta \sim N\Omega/\mathcal{A}^2$ ) in low fields. According to the expectations,  $T_{2,\text{long}}$  depends now on the shape of the wavefunction, i.e. the distribution of  $A_k$  couplings determines now the prefactor multiplying  $N\Omega^2/\mathcal{A}^3$  [H3].

### **Results for the decay of spin echo signal**

The first thing which should be noted is the fact that in a homonuclear system, or a system in which the flip-flops between nuclei of distinct species are forbidden by Zeeman energy mismatch at very high  $B$  fields, the application of SE sequence *completely* removes the influence of the second-order effective Hamiltonian from Eq. (22). It is easy to check that when the interaction term in the Hamiltonian commutes with the Zeeman term, the product of operators under average in Eq. (18) is equal to unity, and thus  $W_{SE}(t) = 1$ . This means that  $\tilde{H}^{(2)}$  can lead to SE decay only at low magnetic fields, at which the inter-species flip-flops start to occur.

<sup>10</sup>I have since then analytically obtained the expression for the sum of all the  $R_k$  at long times, but this result remains unpublished. The analytical formula confirms the results of numerical calculations from [H2,H3].

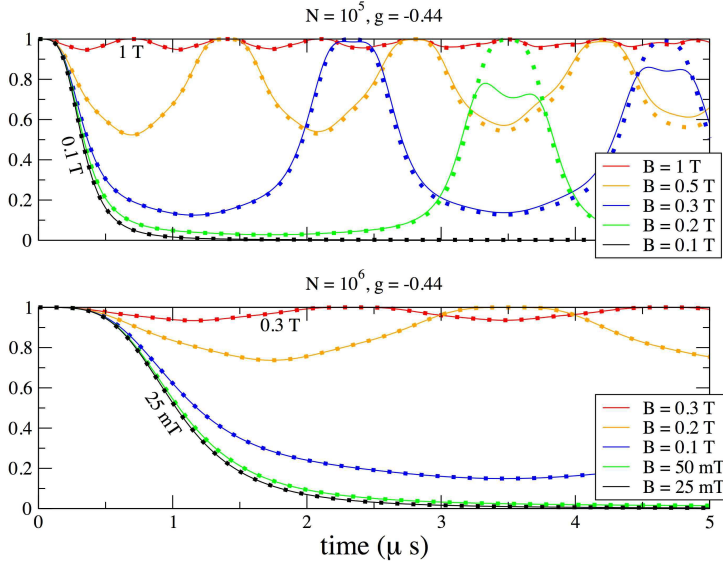


Figure 3: Spin echo decoherence function  $W_{\text{SE}}(t)$  in GaAs. The dots are obtained in the  $A/N \ll \omega_{\alpha\beta}, 1/t$  limit, when  $W(t) = [1 + \frac{1}{2}R_2(t)]^{-1}$ , while the solid lines are the results of the calculation with the  $\tilde{T}$ -matrix large enough to guarantee convergence. The differences between the two approaches on a  $\mu\text{s}$  time-scale are visible for the smaller dot (upper panel,  $N = 10^5$ ), but are negligible for the larger one (lower panel,  $N = 10^6$ ). The figure is adapted from [H2].

Using the above-described formalism it is easy to derive the  $T$ -matrix and expressions for  $R_k$  for the case of SE. At short times and for moderate  $B$  fields, for which  $\omega_{kl} \gg A_{kl}$ , we have the coarse-grained matrix of  $N_J \times N_J$  dimension:

$$\tilde{T}_{\alpha\beta} = (1 - \delta_{\alpha\beta}) \sqrt{a_\alpha a_\beta} \sqrt{n_\alpha n_\beta} \frac{A_\alpha A_\beta}{N\Omega} \frac{2i}{\omega_{\alpha\beta}} e^{i\omega_{\alpha\beta}t/2} \sin^2 \frac{\omega_{\alpha\beta}t}{4}. \quad (37)$$

In GaAs we have  $N_J = 3$ , and a simple calculation of eigenvalues of  $3 \times 3$  matrix leads to the following solution for decoherence function

$$W_{\text{SE}} \approx \frac{1}{1 + \frac{1}{2}R_2(t)}, \quad (38)$$

where

$$R_2(t) = \sum_{\alpha \neq \beta} \frac{4A_\alpha^2 A_\beta^2}{N^2 \Omega^2 \omega_{\alpha\beta}^2} n_\alpha n_\beta a_\alpha a_\beta \sin^4 \frac{\omega_{\alpha\beta}t}{4}. \quad (39)$$

Note that this solution is a result of nontrivial resummation of  $R_k$  of all orders. In the second order of linked cluster (cumulant) expansion we have  $W(t) \approx \exp(-\frac{1}{2}R_2(t))$  (which is the solution given in [56]). The fact that only  $R_2$  appears in Eq. (38) is due to the fact that higher-order  $R_k$  can be expressed in terms of  $R_2$  under the above approximations.

In Fig. 3 there are examples of  $W_{\text{SE}}(t)$  calculated for two GaAs QDs of different sizes ( $N = 10^5$  and  $10^6$ ). At  $B \leq 0.1$  T the signal shows a practically irreversible decay on timescale of a microsecond, consistent with SE measurements performed at such low fields [7]. At slightly higher  $B$  fields one can see the quasi-periodic behavior of the signal. This is somewhat accidental and specific to GaAs, in which the Larmor frequencies of the three isotopes are approximately commensurate. This oscillatory character of the SE signal was the main prediction of [H2,H3]. Almost two years after the appearance of [H2] as a preprint online this prediction was confirmed by experiments on double quantum dots made of GaAs [8].

While the presentation above is focused on general quantum-mechanical theory of decoherence due to hf-mediated interactions, the most striking features of the SE signal (which appear at

short times,  $t \ll N/\mathcal{A}$ ) can be derived using a semiclassical approach [64]. At these short times one can obtain Eqs. (38) and (39) by treating the Overhauser fields coming from distinct nuclear species as classical vectors precessing about the external  $B$  field direction. The classical effective Hamiltonian is of the second order in  $h_x$  and  $h_y$ , which explains the nonlinear mixing of frequencies of precession of distinct nuclear species. Again, this underlines the fact that the RDT applied to  $\tilde{H}^{(2)}$  is a quantum-mechanical generalization of performing Gaussian averages over phases proportional to a square of a random field. Technically, it is the  $1/N$  approximation that leads to “Gaussianization” of the nuclear bath.

#### 4.2.5 Comparison of RDT results with the exact numerics in a system of 20 nuclear spins and dynamics of spin echo signal at very low magnetic fields

Before the predictions of RDT for the SE case were confirmed experimentally, we had performed exact numerical simulations aimed at checking the accuracy of the RDT [H4]. The numerical simulation of a system of an electron and  $N = 20$  nuclear spins was done using the Chebyshev polynomial based method [29]. In the parameter regime in which the RDT was expected to work, i.e. for  $\delta \ll 1$ , we found a good agreement between the exact numerical simulation (taking a few hours of computing time), and the RDT calculation involving only a diagonalization of  $20 \times 20$  matrix. An example of this agreement is shown in Fig. 4, where the exact calculation is compared to RDT using the lowest-order hf-mediated interaction (discussed in detail above), the next order interaction appearing in expansion of  $\tilde{H}_{\text{eff}}$  with respect to  $\hat{V}_{\text{ff}}$  (see [H3] and [H4] for details), and the “pair-correlation approximation” (PCA) or Ref. [56], which amounts to keeping only  $R_2$  in the linked cluster expansion. Note that the oscillations of the SE signal due to nonzero  $\omega_{\alpha\beta}$  in a heteronuclear system are invisible now. This is because the condition of  $\omega_{\alpha\beta} \gg A_{kl}$ , which is fulfilled in a wide range of  $B$  fields in real QDs, and which is necessary for the appearance of a prominent oscillation, is broken here. The RDT is however working very well as long as  $\delta \ll 1$ . Furthermore, the qualitative statement that the SE decay is much stronger in a heteronuclear system compared to a homonuclear system, is seen to hold even at  $\delta = 1$  (i.e. for  $\Omega = 1$  in the units used in these calculations), see Fig. 5.

The results of numerical simulations show that at low  $B$  fields (for  $\delta > 1$ ), the SE signal in a *homonuclear* system exhibits pronounced oscillations with frequency corresponding to Larmor precession frequency  $\omega$  of the nuclei (see the solid lines in Fig. 5). A similar effect is known in the literature under the name of Electron Spin Echo Envelope Modulation (ESEEM) [65–67], and it appears in the presence of *anisotropic* hyperfine interaction between the central spin and the bath spins, i.e. terms of the form  $S^z J^x$ . Although such terms are absent in the Hamiltonian used in the calculations, one can argue that they effectively appear at low  $\Omega$ . Let us focus now on regime of  $\delta \ll 1$ , in which the oscillation is already visible (see the  $\Omega = 2.5$  result in Fig. 5). As discussed before, the random Overhauser field leads to tilting of the electron precession axis away from  $z$  direction by an angle proportional to  $\delta$ , which leads to a rapid suppression of coherence signal by a factor of  $1 - \delta^2$ . This “visibility loss” can be clearly seen in Figures 4 and 5. The physical picture is then the following: the electron spin is precessing with frequency  $\approx \Omega$  about the tilted  $z'$  axis, and this precession is so fast that the influence of the electron spin on the nuclear spins averages out to zero, and the nuclear spins are simply precessing with frequency  $\omega$  about the original  $z$  axis. If we then rotate the coordinate system so that the  $z'$  direction is the electron spin quantization axis, from the original  $AS^z J^z$  Overhauser term we will obtain also the effectively anisotropic term  $\sim S^{z'} J^{x'}$ . In this way the anisotropic hf interaction is dynamically generated during the evolution of a central spin strongly coupled to a nuclear spin bath.

The above semiclassical explanation suggests that the  $\omega$  oscillation should appear in a simplified model in which all the hf couplings  $A_k$  are taken to be the same, all equal to  $A = \mathcal{A}/N$ . This corresponds to a box-shaped wavefunction of the electron. Such a “box” model can be solved exactly under the assumption of the presence of only a single nuclear spin species. The hf Hamiltonian is then given by  $AS \cdot \mathbf{J}$ , with  $\mathbf{J} = \sum_k \mathbf{J}_k$  being the operators of the total spin of the  $N$  nuclei.

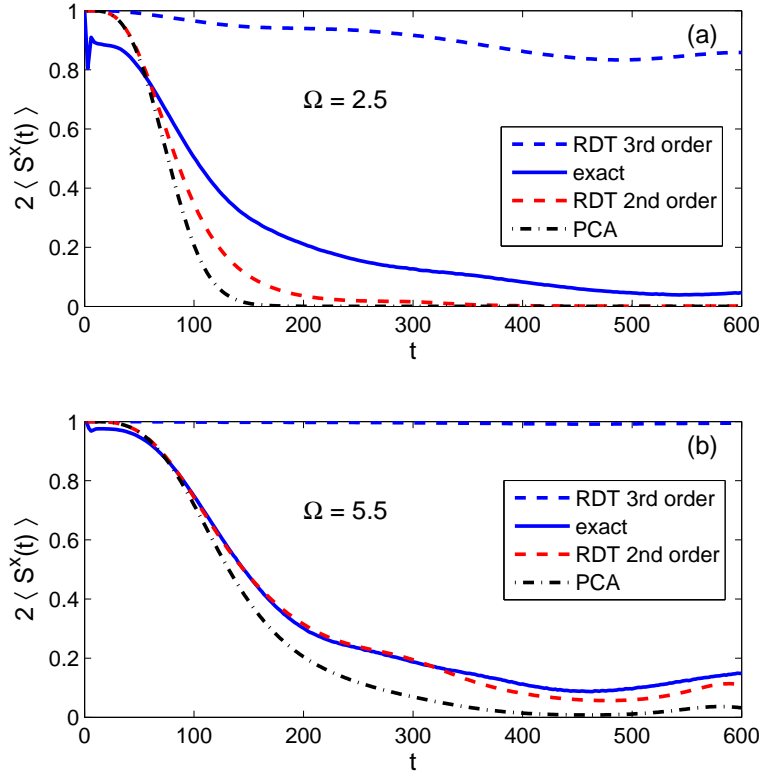


Figure 4: Comparison between the exact (solid line) results for SE signal and the analytical calculations: RDT with the 2nd and 3rd order effective Hamiltonian, and PCA (see text). The units are such that  $\sum_k A_k^2 = 1$  (with randomly chosen  $A_k$  given in [H4]), which means that the unit of  $\Omega$  is  $1/\delta$ , and the unit of time is  $T_2^*/\sqrt{8}$ . The 20 nuclei are divided in three groups (numbering 10, 6, and 4 spins) corresponding to distinct nuclear species with  $\omega_\alpha = 0.02526$ , 0.0354, and 0.045. One can see that the agreement between the RDT calculation employing the 2nd order hf-mediated interaction and the exact result is very good for  $\Omega \gg 1$ . The figure is adapted from [H4].

We can then use the basis of eigenstates of  $\mathbf{J}^2$  and  $J^z$ . In the case of  $J_k = 1/2$  these are the Dicke states well known from quantum optics [68]:  $|\gamma_j, j, m\rangle$  for which  $\mathbf{J}^2 |\gamma_j, j, m\rangle = j(j+1) |\gamma_j, j, m\rangle$  and  $J^z |\gamma_j, j, m\rangle = m |\gamma_j, j, m\rangle$ , and where  $\gamma_j$  is the quantum number specifying the way in which  $N$  spins were added to obtain a state with a given  $j$ . The hf Hamiltonian is diagonal in this  $\gamma_j$  index, and we only need to know the degeneracies  $D_j$  of subspaces associated with given  $j$ . These are given by [69]

$$D_j = \frac{N!}{(N/2 - j)!(N/2 + j)!} \frac{2j + 1}{N/2 + j + 1}. \quad (40)$$

The exact solution is possible because the hf interaction is coupling only pairs of states,  $|\pm, \gamma_j, j, m\rangle$  and  $|\mp, \gamma_j, j, m \pm 1\rangle$ , where the first quantum number corresponds to  $\sigma_z$  eigenvalue of the central spin. The time dependence of the SE signal can thus be obtained by solving for the dynamics in all the two-dimensional subspaces

$$W_{\text{SE}}(t) = \sum_{j=0}^{N/2} \sum_{m=-j}^j \frac{D_j}{2^N} f_{jm}(t), \quad (41)$$

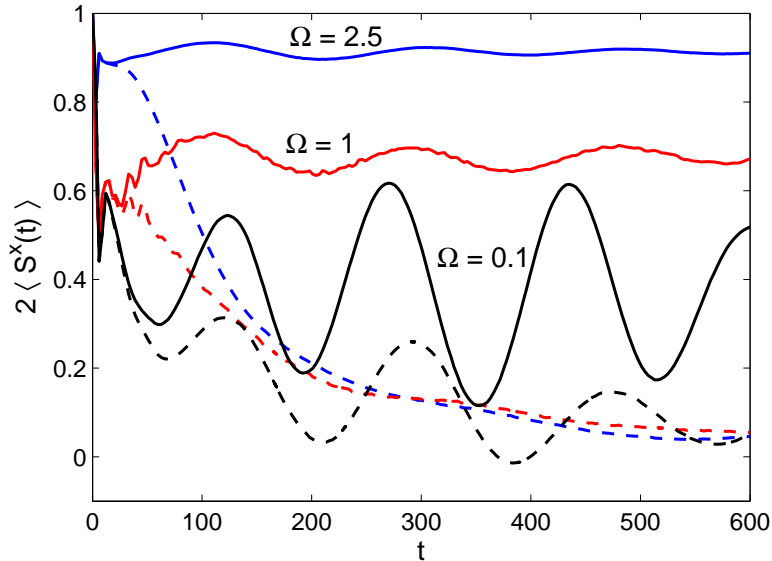


Figure 5: Comparison of the spin echo decay in a heteronuclear bath (dashed lines, parameters as in Fig. 4) and a homonuclear bath (solid lines) with all the bath spins having  $\omega=0.0354$ . The figure is adapted from [H4].

where  $f_{jm}(t)$  is constructed from matrix elements of the evolution operator in two-dimensional subspace, see [H4] for the full formula.<sup>11</sup> The results obtained in this way are in very good agreement with the results of exact numerical simulations even for  $\Omega \ll 1$ , see [H4]. We will revisit the box model in the context of NFID in Section 4.2.7.

#### 4.2.6 Effective Hamiltonian theory of dephasing of two-spin states in double quantum dots

Many experiments on spin control in gated QDs are conducted using double quantum dots (DQDs) containing two electrons. Such a DQD is tuned to  $(1, 1)$  charge state (with  $(n_L, n_R)$  denoting the number of electrons in the left (L) and the right (R) dot), and it is possible to achieve full coherent control in the subspace of singlet ( $S$ ) and unpolarized triplet ( $T_0$ ) states [70]. This two-dimensional subspace forms a logical singlet-triplet (S-T) qubit [6, 10, 14]. In fact the first spin echo measurement in GaAs was done using a DQD [6], and the RDT predictions for SE dynamics at low  $B$  fields were confirmed in a DQD [8]. In this section I will outline the necessary modifications of the previously discussed single-spin theory necessary in the two-electron DQD case, and I will discuss predictions for hf-induced dephasing of superpositions of singlet and triplet states in the regime of large singlet-triplet splitting, which has been addressed experimentally only very recently [25, 71].

The physics of spin state initialization, manipulation, and readout in DQDs is very rich [14], and here let me just mention the basic elements needed to set up a theory of hf dephasing in a relevant logical qubit subspace. The qubit is most naturally initialized in the  $S$  state (but creation of superpositions of  $S$  and  $T_0$  is also possible by adiabatic tuning the system into the ground state of the hyperfine Hamiltonian [71]), and the projection on  $S$  is also the most natural measurement. The  $S$ - $T_0$  splitting,  $\Delta_{ST}$ , is controlled by voltages applied to the two dots. These voltages change energy offset between the single-electron states in the dots, thus affecting the second-order virtual tunneling processes which lower the singlet energy with respect to the triplet

<sup>11</sup>Such a simple solution is impossible in the heteronuclear case, in which we have the hf Hamiltonian given by  $\sum_{\alpha} A_{\alpha} \mathbf{S} \cdot \mathbf{J}_{\alpha}$ . Then, during the evolution starting from a given  $|\sigma_z\rangle \prod_{\alpha} |j_{\alpha}, m_{\alpha}\rangle$  state the relevant subspace is a higher-dimensional space of fixed  $\sigma_z/2 + \sum_{\alpha} m_{\alpha}$ .

energy (this process can be thought as related to superexchange, only with doubly-occupied state in one of the dot playing the role of the intermediary state), and they can also influence the overlap between the orbitals in the two dots, thus affecting the direct exchange contribution to the  $S$ - $T_0$  splitting. The rotations between  $S$  and  $T_0$  states require the presence of controlled gradient of the  $z$  component of the magnetic field. Very often it is the difference of the average  $z$  component of the Overhauser field in the two dots (when the nuclei in the two dots were previously polarized by some means) which is used for qubit manipulation [10, 70].

We are interested in the subspace spanned by the lowest-energy orbitals in the two dots, under the constraint of (1, 1) charge occupation. The four states in this subspace are the singlet,  $|S\rangle = \psi_S \otimes (|\uparrow\downarrow\rangle - |\downarrow\uparrow\rangle)/\sqrt{2}$ , and triplet states  $|T_{+,0,-}\rangle = \psi_{AS} \otimes |\uparrow\uparrow\rangle, (|\uparrow\downarrow\rangle + |\downarrow\uparrow\rangle)/\sqrt{2}$ , and  $|\downarrow\downarrow\rangle$ . The orbital parts  $\psi_{S/AS}$  are symmetric and antisymmetric combinations of  $\Psi_L(\mathbf{r})$  and  $\Psi_R(\mathbf{r})$  states, which are the single-electron ground state orbitals of the potentials for the L and R dots. The hf interaction is given by

$$\hat{H}_{hf} = \sum_i \mathcal{A}_{\alpha[i]} \mathbf{S}_1 \cdot \mathbf{J}_i \nu_0 \delta(\mathbf{r}_1 - \mathbf{R}_i) + \sum_i \mathcal{A}_{\alpha[i]} \mathbf{S}_2 \cdot \mathbf{J}_i \nu_0 \delta(\mathbf{r}_2 - \mathbf{R}_i), \quad (42)$$

where  $\mathbf{S}_{1,2}$  are the spin operators of the two electrons at positions  $\mathbf{r}_{1,2}$ , and  $\mathbf{J}_i$  are the spin operators of nuclei at site  $\mathbf{R}_i$ . Projecting Hamiltonian (42) onto the  $\{S, T_0, T_+, T_-\}$  basis, we obtain [72, 73] the total electronic and hf Hamiltonian:

$$\hat{H}_e + \hat{H}_{hf} = \begin{pmatrix} -\Delta_{ST} & \theta_T & 0 & 0 \\ \theta_T & 0 & 0 & 0 \\ 0 & 0 & -\mu_T & 0 \\ 0 & 0 & 0 & \mu_T \end{pmatrix} + \begin{pmatrix} 0 & \delta\hat{\theta} & -\sum_i \frac{B_i}{\sqrt{2}} J_i^+ & \sum_i \frac{B_i}{\sqrt{2}} J_i^- \\ \delta\hat{\theta} & 0 & \sum_i \frac{C_i}{\sqrt{2}} J_i^+ & \sum_i \frac{C_i}{\sqrt{2}} J_i^- \\ -\sum_i \frac{B_i}{\sqrt{2}} J_i^- & \sum_i \frac{C_i}{\sqrt{2}} J_i^- & \delta\hat{\mu} & 0 \\ \sum_i \frac{B_i}{\sqrt{2}} J_i^+ & \sum_i \frac{C_i}{\sqrt{2}} J_i^+ & 0 & -\delta\hat{\mu} \end{pmatrix}, \quad (43)$$

In the above Hamiltonian  $B_i = \frac{1}{2}(A_i^L - A_i^R)$  and  $C_i = \frac{1}{2}(A_i^L + A_i^R)$  with  $A_i^{L/R} = \mathcal{A}_{\alpha[i]} |\Psi_{L/R}(\mathbf{r})|^2$ , the total effective field gradient is  $\theta_T$ , the total average field is  $\mu_T$ , and the terms corresponding to fluctuations about these average values are  $\delta\hat{\theta} \equiv \sum_i B_i (I_i^z - \langle I_i^z \rangle)$  and  $\delta\hat{\mu} \equiv \sum_i C_i (I_i^z - \langle I_i^z \rangle)$ .

We derive then an effective Hamiltonian in the  $S$ - $T_0$  subspace, valid when the coupling to  $|T_{\pm}\rangle$  states (given by the typical magnitude of the transverse Overhauser field difference between the dots,  $\sigma_{\perp}$ ) is much smaller than the energy splitting between  $S$ ,  $T_0$  and the polarized triplets:  $\sigma_{\perp} \ll |\Delta_{ST} \pm \mu_T|, |\mu_T|$ . Using the appropriate canonical transformation one derives a set of somewhat complicated second-order hyperfine terms affecting both the  $S$ - $T_0$  energy splitting, and the mixing of  $S$  and  $T_0$ . Let me summarize here the main results without giving all the rather boring details.

### Uncoupled dots

At  $\Delta_{ST}=0$  the two dots are uncoupled, and the electron spins are independent. It is then more convenient to rewrite the Hamiltonian in the basis of  $|\pm X\rangle = \frac{1}{\sqrt{2}}(|S\rangle \pm |T_0\rangle) = \{|\uparrow\downarrow\rangle, |\downarrow\uparrow\rangle\}$  states. The resulting Hamiltonian is of the pure dephasing form:

$$\hat{H} \approx (\hat{V}_H + \theta_T + \delta\hat{\theta})(|+X\rangle \langle +X| - |-X\rangle \langle -X|). \quad (44)$$

where

$$\hat{V}_H = -\frac{1}{8\mu_T} \sum_{i,j} (A_i^L A_j^L - A_i^R A_j^R) (J_i^+ J_j^- + J_i^- J_j^+). \quad (45)$$

The initialization of the  $S$  state at  $\Delta_{ST}=0$  can be then viewed as initialization of superposition of  $|\pm X\rangle$  states which are then subjected to pure dephasing due to the first-order and second-order hyperfine terms. In a free evolution experiment (with long data acquisition time) the ensemble coherence will decay in  $T_2^* \approx 1/\sigma_z$  due to the  $\delta\hat{\theta}$  term [6, 9] ( $\sigma_z$  is the standard deviation of the difference of longitudinal components of the Overhauser fields in the two dots).

On the other hand, in a Hahn echo experiment [6, 8] the influence of  $\delta\hat{\theta}$  is removed, and the signal decay is due to  $\hat{V}_H$  from Eq. (45). Since this interaction is a sum of two commuting terms from two uncoupled dots, the appropriately defined  $S$ - $T_0$  decoherence function is a product of the two single-dot decoherence functions [8, 64]. This observation establishes the correspondence between single-spin Hahn echo decay [7] due to hf-mediated interactions described in previous sections, and the  $\Delta_{ST}=0$  singlet-triplet Hahn echo decay [6, 8]. The theory from [H2,H3] applies to this case, with the only modification being the replacement of  $W(t)$  function by a product of two such functions corresponding to single-spin dephasing in each of the dots.

### The case of $\Delta_{ST} > 0$ , no interdot field gradient

At  $\Delta_{ST} \gg \sigma_z, \sigma_\perp$  we consider the decoherence of a superposition of  $|S\rangle$  and  $|T_0\rangle$ . In the absence of the effective interdot field gradient  $\theta_T$  we can perform another canonical transformation and arrive at an effective Hamiltonian diagonal in  $\{S, T_0\}$  basis. The main observation is that the terms linear in the Overhauser field, which were the cause of very fast  $T_2^*$  decay for a single spin, are strongly suppressed by finite  $\Delta_{ST}$ . The dephasing of a  $S$ - $T_0$  superposition occurs due to the second-order terms which are suppressed by  $1/\Delta_{ST}$  or  $1/\mu_T$ . The investigation presented in [H7] showed that in GaAs and Si DQDs there are two potentially important channels of hf-related dephasing. The first is due to the  $\hat{H}_A \hat{\tau}_z$  term (with  $\hat{\tau}_z$  being the third Pauli matrix in the basis of  $\{S, T_0\}$ ), in which

$$\hat{H}_A = -\frac{1}{\Delta_{ST}} \sum_{i,j} B_i B_j J_i^z J_j^z = -\frac{\delta\hat{\theta}^2}{\Delta_{ST}}. \quad (46)$$

As discussed before we can treat  $\theta = (h_L^z - h_R^z)/2$  as a Gaussian random variable, and we obtain the relevant decoherence function  $W_A(t)$  by evaluating the Gaussian integral:

$$W_A(t) = \int \frac{1}{\sqrt{2\pi}\sigma_\theta} e^{-2\frac{\theta^2}{\sigma_\theta^2}} e^{2i\theta^2 t/\Delta_{ST}} d\theta = \frac{e^{\frac{i}{2} \arctan(\eta_A t)}}{(1 + \eta_A^2 t^2)^{1/4}}, \quad (47)$$

where we have defined  $\eta_A = \sigma_z^2/\Delta_{ST}$ . The characteristic decay time scale  $T_A$  is defined by  $|W_A(T_A)| = 1/e$ , giving us

$$T_A = \frac{e^2 \Delta_{ST}}{\sigma_z^2} = \frac{e^2 N_D \Delta_{ST}}{n_F^2 \mathcal{A}^2}, \quad (48)$$

where  $N_D = (N_L^{-1} + N_R^{-1})^{-1}$  and  $n_F \leq 1$  is the factor accounting for possible narrowing of the distribution of the Overhauser field difference.

The second important dephasing channel is due to a term  $\hat{V}_{SS} |S\rangle \langle S|$ , which comes from the virtual flip flops between  $S$  and  $T_\pm$ :

$$\hat{V}_{SS} = \frac{\Delta_{ST}}{\mu_T^2 - \Delta_{ST}^2} \sum_{i,j} B_i B_j J_i^+ J_j^- = v_{ss} \sum_{i,j} (A_i^L A_j^L + A_i^R A_j^R - A_i^L A_j^R - A_i^R A_j^L) J_i^+ J_j^-, \quad (49)$$

with  $v_{ss} = \Delta_{ST}/4(\mu_T^2 - \Delta_{ST}^2)$ . Since this is the second-order hf-mediated inter-nuclear flip-flop interaction, it can be treated with the RDT. The calculations are very similar to the ones discussed previously in the case of NFID of a single spin (but note that now we do not have to assume any narrowing). At short times we obtain

$$W_{SS}(t \ll 1/\omega_{\alpha\beta}) \approx \frac{e^{-i \arctan(\eta_{SS} t)}}{\sqrt{1 + (\eta_{SS} t)^2}}, \quad (50)$$

where

$$\begin{aligned} \eta_{SS} &= |v_{ss}| \left( \sum_{k \in L} a_k A_k^2 + \sum_{k \in R} a_k A_k^2 \right) \\ &= 2|v_{ss}| (\sigma_{\perp,L}^2 + \sigma_{\perp,R}^2) \equiv 2|v_{ss}| \sigma_\perp^2. \end{aligned} \quad (51)$$

These equations should be compared with Eq. (31) obtained before. The characteristic decay timescale is

$$T_{SS} = \frac{\sqrt{e^2 - 1}}{2v_{ss}} \frac{1}{\sigma_{\perp}^2} = 2\sqrt{e^2 - 1} \frac{|\mu_{\text{T}}^2 - \Delta_{\text{ST}}^2|}{\Delta_{\text{ST}}\sigma_{\perp}^2}. \quad (52)$$

The main thing to notice here is that these two mechanisms have opposite dependence on  $\Delta_{\text{ST}}$ . Dephasing due to  $\hat{H}_A$  is weaker at larger  $\Delta_{\text{ST}}$ , since this term in the effective Hamiltonian comes from the second order contribution of the  $\delta\hat{\theta}$  term (mixing of  $S$  and  $T_0$ ), which is suppressed by finite  $\Delta_{\text{ST}}$ . On the other hand, the  $\hat{V}_{SS}$  term is enhanced at larger  $\Delta_{\text{ST}}$ . This term is a sum of two contributions, corresponding to two different second-order virtual transitions, one involving  $|T_+\rangle$  and the other  $|T_-\rangle$ . At  $\Delta_{\text{ST}} = 0$  there is a destructive interference between these paths, and  $\hat{V}_{SS}$  disappears, while at  $\Delta_{\text{ST}} \rightarrow |\mu_{\text{T}}|$  the strength of this interaction increases due to the small energy denominator for one of the virtual transitions. As a consequence of this contrasting behavior of the two dephasing mechanisms, the dephasing time has a maximum at  $\Delta_{\text{ST}} \approx 0.64\mu_{\text{T}}$  (assuming  $\sigma_{\perp} = \sigma_z$ ).

### The case of $\Delta_{\text{ST}} > 0$ with the interdot field gradient

In the presence of a finite field gradient  $\theta_{\text{T}} \gg \sigma_z$  one needs to obtain the new eigenstates that account for the  $\theta_{\text{T}}$ -induced mixing of  $S$  and  $T_0$ , and then to re-derive the pure dephasing Hamiltonian in the new eigen-basis. The mixing of  $S$  and  $T_0$  states means that the electron spin density in each dot does not vanish anymore. As such the linear longitudinal Overhauser field,  $\delta\hat{\theta}$ , leads to dephasing between the eigenstates, similar to what happens to single spin qubits. Indeed, if  $\theta_{\text{T}} \gg J$ , the eigenstates approach the product states again, so that we recover the case of dephasing of two independent spins.

Although there are many terms present in the transformed effective Hamiltonian, the analysis of their influence given in [H7] shows that for almost all possibly relevant values of parameters the  $S$ - $T$  coherence time for  $\theta_{\text{T}} \gg \sigma_z$  is given by

$$T_{2,\theta_{\text{T}}}^* = \frac{1}{|\sin 2\gamma|} \frac{\sqrt{2}}{\sigma_z} \approx \frac{\sqrt{2}\Delta_{\text{ST}}}{4\sigma_z\theta_{\text{T}}}, \quad (53)$$

where we used the mixing angle defined by  $\tan 2\gamma = -\frac{2\theta_{\text{T}}}{\Delta_{\text{ST}}}$ . When  $\gamma$  approaches  $\pi/4$  (i.e.,  $\theta_{\text{T}} \gg \Delta_{\text{ST}}$ ),  $T_{2,\theta_{\text{T}}}^*$  approaches the  $T_2^* \sim 1/\sigma_z$  for a single spin in a QD. One can see that the use of substantial  $\theta_{\text{T}}$  gradient, while allowing for full control over the  $S$ - $T_0$  qubit, leads to strong inhomogeneous dephasing similar to the case of a single spin.

This inhomogeneous broadening is of course removed by the echo sequence, which in the case of  $S$ - $T_0$  superposition is effected by tuning  $\Delta_{\text{ST}}$  to zero at the mid-point of the evolution for a time in which the  $\theta_{\text{T}}$  term rotates the qubit by  $\pi$ . The calculations of the resulting echo signal decay due to the presence of the second-order hf terms (such as  $\hat{V}_{SS}$ ) are given in [H7]. The calculated signals again exhibit characteristic oscillations due to the presence of multiple nuclear species. However, the comparison of calculations with the recent experiments on such singlet-triplet echo [25] shows that the hf-induced dephasing is not the dominating source of decoherence. It appears that classical charge noise leading to fluctuations of  $\Delta_{\text{ST}}$  is limiting the coherence time of superposition of  $S$  and  $T_0$  states. The characteristics of this noise, which acts locally on a nanoscale structure forming the qubit, can only be read out from the measured coherence dynamics of the qubit. In Chapter 4.3 I will discuss how such a characterization can be achieved.

#### 4.2.7 Comparison of the RDT with the Nakajima-Zwanzig generalized Master equation approach

While the RDT predictions for spin echo decay were quickly confirmed experimentally, giving strong support to this theory, the existing NFID measurements [50] are not detailed enough to

allow for quantitative comparison with other theories. Such a comparison would be interesting, since the theory of NFID decay based on Nakajima-Zwanzig (NZ) generalized Master equation (GME) approach, which has been developed since 2004 [11, 12, 74], gives predictions at moderate values of  $\Omega$  which are distinct [12] from the predictions of RDT [H2,H3]. It is important to note that in this theory one uses the *full* hf Hamiltonian, and performs the expansion explicitly in powers of the flip-flop term,  $\hat{V}_{\text{ff}}$ . This has to be contrasted with the RDT, which is based on the effective Hamiltonian, and the expansion is in powers of the electron-mediated interaction. The paper [H6] was written with the aim of shedding some light on relation between these two approaches.

The calculations from [H6] are much more technical (and, in my opinion, much less transparent) than the linked cluster and  $1/N$  expansions used in derivations of RDT. The main problem is that the NZ approach does not have any simple connection to a well-known diagrammatic perturbation theory technique, and one has to painstakingly generate the expansion order by order, with only the 4th order expansion being carried out exactly in the literature, and with partial results for higher orders briefly discussed in [12]. This should be contrasted with the structure of RDT which allowed for infinite-order resummation of the linked cluster expansion. Because of the technicality of derivations from [H6], below I will focus only on the important qualitative conclusions of this paper.

The long-time dynamics (both in NZ theory and in RDT) is crucially affected by the shape of the wavefunction. We have decided to focus on the short-time regime, in which this shape should be irrelevant. We have thus worked on NFID within the box wavefunction (uniform hf coupling,  $A_k = A \equiv \frac{A}{N}$ ) model. In this case, as I discussed previously for the SE, it is possible to derive an exact solution, in which  $W(t)$  is expressed as a sum over  $\sim N$  oscillatory functions, all of which can be obtained from analytical diagonalization of  $2 \times 2$  matrices.

The NZ approach is based on separation of the total density matrix into a relevant and “irrelevant” part [75, 76]:  $\rho = \rho_{\text{rel}} + \rho_{\text{irrel}}$ . In applications where one considers the dynamics of a system coupled to a bath,  $\rho_{\text{rel}}$  is typically a density matrix describing the degrees of freedom of the system. This partition is implemented by introducing projection superoperators  $P$  and  $Q$  such that

$$P\rho = \rho_{\text{rel}}, \quad Q\rho = \rho_{\text{irr}}, \quad P + Q = \mathbf{1}, \quad PQ = 0. \quad (54)$$

The Liouville equation for  $\rho$  can then be transformed into an exact equation for the evolution of  $\rho_{\text{rel}}$ :

$$P\dot{\rho}(t) = -iPLP\rho(t) - i \int_0^t dt' \hat{\Sigma}(t-t')P\rho(t'), \quad (55)$$

where

$$\hat{\Sigma}(t) \equiv -iPLQe^{-iLQt}QLP. \quad (56)$$

The Liouvillian superoperator  $L$  implements the evolution of the total system and is defined to act on an arbitrary operator  $\mathcal{O}$  according to  $L\mathcal{O} = [H, \mathcal{O}]$ . The superoperator  $\hat{\Sigma}$  is referred to as the memory kernel, or sometimes as the self-energy (although I consider the use of this term inappropriate for the reasons explained below).

The operator  $P$  used in [11, 12, 74] was defined by

$$P\rho = \rho_J(0) \otimes \text{Tr}_J\rho = \rho_J(0) \otimes \rho_e. \quad (57)$$

It is however crucial to note that this is not the only possible choice. It is possible to instead define  $P$  as a sum over many projection operators which project onto various subspaces of the nuclear bath state space, and the choice of  $P$  can strongly influence the convergence properties of the resulting theory [77, 78]. In fact, we will see in a moment that in the context of the box model that the choice made in Eq. (57) is far from ideal. For now we will use the choice from [11, 12, 74].

Calculating the expectation value of  $S^+$  operator (which is proportional to  $W^*(t)$ ) we arrive at

$$\frac{d}{dt}\langle S^+(t) \rangle = i\Omega_n \langle S^+(t) \rangle - i \int_0^t dt' \Sigma(t-t') \langle S^+(t') \rangle, \quad (58)$$

where  $\Omega_n \equiv \Omega + h_n^z$ , where  $h_n^z$  is the value of the longitudinal Overhauser field in the narrowed state. The memory kernel is now a function instead of an operator:

$$\Sigma(t) \equiv -i \text{Tr} [S^+ PLQ e^{-iLQt} QLPS^- \rho_I(0)]. \quad (59)$$

Eq. (58) is an integro-differential equation which can be solved by performing a Laplace transform, after which the equation becomes algebraic with the solution

$$\langle S^+(s) \rangle = \int_0^\infty dt e^{-st} \langle S^+(t) \rangle = \frac{\langle S^+(t=0) \rangle}{s - i\Omega_n + i\Sigma(s)}. \quad (60)$$

The solution in the time domain is then obtained by computing the Bromwich inversion integral,

$$\langle S^+(t) \rangle = \frac{1}{2\pi i} \int_{\gamma-i\infty}^{\gamma+i\infty} ds e^{st} \langle S^+(s) \rangle, \quad (61)$$

where the contour defined by the real number  $\gamma$  must be chosen such that it lies to the right of all the poles of  $\langle S^+(s) \rangle$ . Therefore, solving for  $\langle S^+(t) \rangle$  requires solving for the Laplace transform of the memory kernel:

$$\Sigma(s) = \int_0^\infty dt e^{-st} \Sigma(t) = -i \text{Tr} \left[ S^+ PLQ \frac{1}{s + iLQ} QLPS^- \rho_J(0) \right], \quad (62)$$

Computing  $\Sigma(s)$  exactly is a difficult perturbative problem, because there is in fact no diagrammatic representation of terms which appear in perturbative expansion (thus calling  $\Sigma(s)$  the ‘‘self energy’’ is inappropriate, since real self-energy is defined as a sum over properly defined irreducible diagrams). Following [11, 12, 74] we have proceeded by expanding the memory kernel in powers of the flip-flop interaction  $\hat{V}_{\text{ff}}$ . The details of this very cumbersome expansion (carried out to the 4th order) are given in [H6]. Here I will simply present Figure 6, in which the 4th order NZ solution is compared with the exact box model solution. The disagreement is very clear.

However, it was shown in Ref. [77] that the standard projection operator is far from being the best possible choice for the Hamiltonian which exhibits a significant degree of symmetry. When symmetries are present, one can instead replace  $P$  with a series of so-called *correlated* projection (CP) operators which project onto invariant subspaces of state space, enabling one to expand the reduced density matrix for the system as a sum of matrices, each capturing the components of the state lying in a particular subspace. In the uniform coupling model it is natural to define the operators  $\Pi_{jm}$  on subspaces of fixed  $j$  and  $m$ . We choose now the projector  $P$  as

$$P\tilde{\rho} = \sum_{jm} \text{Tr}_J(\Pi_{jm}\tilde{\rho}) \otimes \frac{1}{D_j} \Pi_{jm} \equiv \sum_{jm} \tilde{\rho}_e^{jm} \otimes \frac{1}{D_j} \Pi_{jm}. \quad (63)$$

The  $\tilde{\rho}_e^{jm}$  are a set of matrices which sum to give the reduced density matrix for the electron spin:

$$\tilde{\rho}_e = \sum_{jm} \tilde{\rho}_e^{jm} = \sum_{m=-N/2}^{N/2} \sum_{j=|m|}^{N/2} D_j \tilde{\rho}_e^{jm}. \quad (64)$$

As shown in [H6], even only in the 2nd order of expansion with respect to  $\hat{V}_{\text{ff}}$ , the NZ theory using these correlated projectors gives results in very good agreement with the exact solution, see Figure 7.

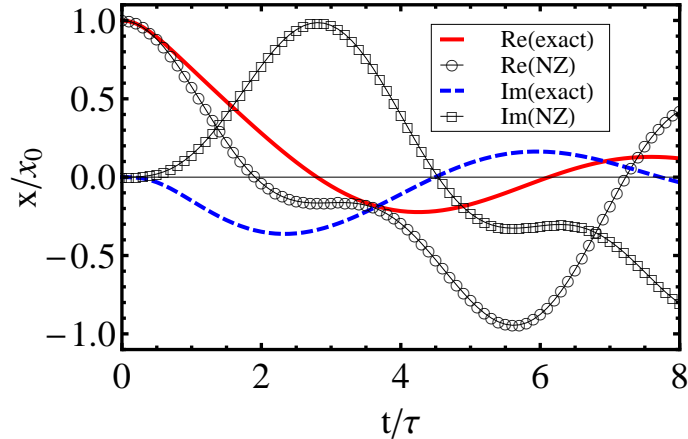


Figure 6: Exact solution of the uniform coupling model vs. NZ GME result for  $\mathcal{A} = \Omega$ , and  $h^z = 0$ . The time unit  $\tau = 4\Omega_n N/\mathcal{A}^2$ . The plotted quantity  $x(t)/x_0$  is equal to  $W^*(t)$  evaluated in the rotating frame in which the fast precession due to magnetic field splitting is absent. The Figure is adapted from Ref. [H6].

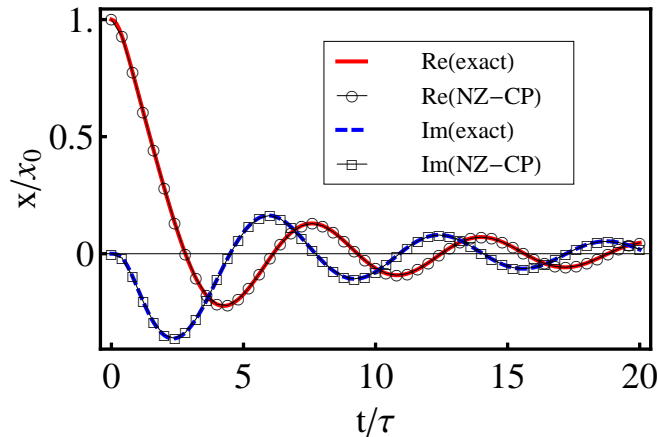


Figure 7: Exact solution of the uniform coupling model vs. NZ GME result with correlated projectors result for  $\mathcal{A} = \Omega$  and  $h^z = 0$ . The Figure is adapted from Ref. [H6].

Let us finally compare the exact box model solution with the RDT solution. The short-time NFID result from Eqs. (31) and (32) turns out to be practically indistinguishable from the exact result - the RDT results in Fig. 7 would lie exactly on top of the other lines. The only difference between the RDT and the exact (or second-order NZ-CP) calculations is the lack of a very small-amplitude ( $\sim \delta^2$ ) oscillation on top of the envelope shown in the Figures here. The analytical relation between the RDT solution and the exact solution is discussed in [H6].

These results show that the regime of low magnetic fields is very hard to access by the standard NZ theory. With lowering of  $\Omega$ , the decoherence time is expected to become shorter. On the other hand, there has to be a timescale at which the time-energy uncertainty principle allows one to disregard the exact shape of the wavefunction (i.e. the details of distribution of hf couplings). The simplest guess for this timescale is  $N/\mathcal{A}$ , and RDT calculation agrees with this guess. The NZ calculations from [12] suggest that at low fields and *long times*,  $t \gg N/\mathcal{A}$ , RDT fails at correctly describing the NFID decay. We have shown that, on the other hand, the standard NZ theory carried out to finite order of expansion in  $\hat{V}_{\text{ff}}$ , must fail at describing the nontrivial short-time dynamics of NFID at low  $\Omega$ . The two theories seem therefore to be complementary, and the regions of parameters (magnetic fields and timescale) in which neither

is fully controlled should be further investigated with other methods. Finally, let me note that the considerations on the possible reasons for failure of the standard NZ method in the box case contained in [H6], led us to the conclusion that the so-called time-convolutionless generalized master equation [76] is a better approach to the central spin problem. Recently we published a paper [79] in which this method was used to calculate NFID at short times for a polarized nuclear bath, with zero-polarization result reproducing the RDT formulas.

### 4.3 From coherence measurements to effective description of the environment: noise spectroscopy with qubits

Until now we were focusing on a theory of decoherence in the situation in which the microscopic (and nontrivial) Hamiltonian of the bath is known. However, very often the only information that we have about the local environment of the qubit comes from the measurements of the qubit's dynamics. Of course usually we can make some guesses about the nature of the environment. In the case of solid-state based qubits there are, for example, many known sources of charge noise such as fluctuating electric dipoles omnipresent in insulating materials, or charge traps. Their presence is expected, but their detailed properties (the number of sources close to the qubit, characteristic timescales of fluctuations etc) are sample-dependent. Also, very often it is simply not known what is the relevant bath: it could be phonons, charge fluctuations, magnetic field fluctuations caused by magnetic impurities, etc. Finally, the qubit is affected by its *local* environment, (the effective size of which depends on the time-scale of interest, with the remote parts of the environment not having a large influence at short times), which often cannot be characterized with independent methods. All these are motivations for trying to invert the problem of qubit-environment interaction: instead of calculating the qubit's decoherence due to the dynamics of a given bath, we will try to learn something about the unknown environment by analyzing the measurements of qubit's decoherence.

Of course we must assume something about the environment. While qubit's relaxation [20, 30, 80] is affected by bath fluctuations with frequencies  $\sim \Omega$  (the qubit's energy splitting), the *dephasing* of the qubit is typically dominated by low-frequency environmental fluctuations. When the bath temperature is larger than the energy scale of these low-energy excitations, the two-point correlation functions of the bath degrees of freedom have classical behavior [80]. Below we will focus on environment-induced dephasing of the qubits, and we will assume that the influence of this environment can be mapped on qubit's interaction with a source of classical noise  $\xi(t)$ . Furthermore, we will assume that this noise is stationary and (in most cases) that it has Gaussian statistics, i.e. it is fully characterized by its two-point correlation function,  $C(t-t') = \langle \xi(t)\xi(t') \rangle$ , or, equivalently, by its spectral density defined by

$$S(\omega) = \int_{-\infty}^{\infty} C(t)e^{i\omega t} dt . \quad (65)$$

In [H1] we focused on the case of qubits based on superconducting circuits, for which the strong influence of classical charge and flux noise had been already widely recognized. However, later it became clear that the domain of applicability of this approach is much wider. For example, DQD based spin qubits are strongly affected by charge noise (voltage fluctuations on the gates, fluctuations of local electric fields caused by charge traps) when singlet-triplet splitting  $\Delta_{ST}$  is not zero. Even single-spin qubits turned out to be affected by charge noise: fluctuating electric fields affect the position and the shape of the electron's wavefunction, which leads to spin dephasing via spin-orbit coupling or because the Overhauser field felt by the electron becomes time-dependent due to such fluctuations (which lead to time-dependence of  $A_k$  couplings).

Below I will present the overview of results of [H1] and [H8] for, respectively, the cases of linear coupling to the noise (i.e.  $v_1\xi(t)\hat{\sigma}_z$  coupling) and the quadratic coupling (i.e.  $v_2\xi^2(t)\hat{\sigma}_z$ ). These are the two situations most often encountered in experiments.

### 4.3.1 Linear coupling to classical noise

For a Gaussian process  $\xi(t)$  the average over the realizations of the process is a Gaussian functional integral

$$\langle \dots \rangle = \int \mathcal{D}[\xi(t)] \exp \left( -\frac{1}{2} \int dt_1 \int dt_2 \xi(t_1) C^{-1}(t_1 - t_2) \xi(t_2) \right) \dots, \quad (66)$$

where  $C^{-1}$  is defined by

$$\int C^{-1}(t - t'') C(t'' - t') dt'' = \delta(t - t'). \quad (67)$$

We focus on the dynamics of the off-diagonal element of qubit's density matrix when the qubit is subjected to a sequence of ideal  $\pi$  pulses leading to Dynamical Decoupling (DD) of the qubit from the environment [44–46]. The decoherence function is then given by

$$W(t) = \langle e^{-iv_1 \int \xi(t') f_t(t') dt'} \rangle, \quad (68)$$

where  $f_t(t')$  is the time-domain filter function characterizing the DD sequence that we have already encountered (see Fig. 1 for examples). The Gaussian average can be easily performed using the standard methods, and we obtain

$$W(t) = e^{-\chi(t)} \quad \text{with} \quad \chi(t) = v_1^2 \int_0^\infty \frac{d\omega}{2\pi} S(\omega) |\tilde{f}_t(\omega)|^2 = v_1^2 \int_0^\infty \frac{d\omega}{\pi} S(\omega) \frac{F(\omega t)}{\omega^2}, \quad (69)$$

where  $\tilde{f}_t(\omega)$  is the Fourier transform of  $f_t(t')$  with respect to  $t'$ . The filter function  $F(\omega t) = \frac{\omega^2}{2} |\tilde{f}_t(\omega)|^2$  encapsulates the influence of the pulse sequence on decoherence [81]. In terms of times  $t_k$  at which the pulses are applied (with  $t_0=0$  and  $t_{n+1}=t$ ) we have

$$F(\omega t) = \frac{1}{2} \left| \sum_{k=0}^n (-1)^k (e^{i\omega t_{k+1}} - e^{i\omega t_k}) \right|^2. \quad (70)$$

In the case of free evolution of the qubit we have

$$F_{\text{FID}}(\omega t) = 2 \sin^2 \frac{\omega t}{2}, \quad (71)$$

which leads to

$$\chi_{\text{FID}}(t) = v_1^2 \int_0^\infty \frac{d\omega}{\pi} S(\omega) \frac{2 \sin^2 \frac{\omega t}{2}}{\omega^2} \approx \frac{v_1^2 t^2}{2} \int_0^\infty \frac{d\omega}{\pi} S(\omega) \equiv \frac{\sigma^2 t^2}{2} \equiv \left( \frac{t}{T_2^*} \right)^2, \quad (72)$$

where in the second expression we assumed that the integral is dominated by low-frequency part of  $S(\omega)$  (i.e. by  $S(\omega)$  with  $\omega$  up to  $\approx 1/t$ ), and then we extended the limit of integration again to  $\infty$ .  $\sigma^2$  above is the total power of the  $v_1 \xi(t)$  noise. The above calculation is self-consistent if the resulting  $T_2^*$  time is so short that the total noise power is indeed well approximated by integral of  $S(\omega)$  up to  $1/T_2^*$ . Note that the resulting decay is the *not* due to fluctuations which occur during qubit's evolution, but due to slow fluctuations which occur *between* the repetitions of the qubit's initialization-evolution-measurement cycle. We thus again encounter the case of inhomogeneous broadening which can be described using a quasi-static bath approximation.

The case of  $1/f$  type noise will be relevant below, so let us mention that for  $S(\omega) \propto 1/\omega$  the  $T_2^*$  time acquires a logarithmic dependence on the low-frequency (infrared) cutoff of the noise:  $\chi(t) \propto t^2 \ln 1/\omega_0 t$ . In most cases in which such noise appears, no sign of intrinsic infrared cutoff has been found, and the cutoff  $\omega_0$  is in fact given by the inverse of the total data acquisition time:  $\omega_0 \approx 1/T_M$ . For noise with  $S(\omega) \propto 1/\omega^\beta$  with  $\beta > 1$  we have then  $T_2^* \propto 1/T_M^{(\beta-1)/2}$ .

As discussed before, the application of the echo sequence removes the quasi-static shifts of qubit's frequency. Formally we have

$$F_{\text{SE}}(\omega t) = 8 \sin^4 \frac{\omega t}{4}, \quad (73)$$

and one can see, after plugging the above into Eq. (69) that the contribution of low-frequency noise to  $\chi(t)$  is strongly suppressed, even for  $1/\omega^\beta$  noise, provided that  $\beta < 2$ .

Multipulse DD sequences act as even more efficient high-pass filters of the environmental noise. In [H1] we have analyzed the dephasing under the influence of the classical CPMG sequence, the periodic application of pulses (PDD), the sequences based on concatenations of the echo sequence (CDD developed in [45]), and the UDD sequence proposed by Uhrig [46], which fulfills the following optimality condition: for  $n$  applied pulses the first  $2n + 1$  terms in time expansion of  $\chi(t)$  about  $t=0$  are zero, and  $F(\omega t) \propto (\omega t)^{2n+2}$  for  $\omega t \ll 2$ . For comparison, CPMG sequence with even (odd)  $n > 1$  gives the frequency filter  $F(z) \propto z^6$  ( $z^4$ ) for  $z \ll 1$ . Interestingly, this difference between low-frequency suppression for even and odd  $n$  in this sequence was shown to have measurable consequences for  $1/\omega^\beta$  noise with  $\beta > 2$  [82] (see the description of research not included in the habilitation thesis).

The main results of [H1] for the case of Gaussian noise are

- The “optimal” UDD sequence gives the best protection against dephasing only when the noise spectrum has a hard high-frequency cutoff  $\omega_c$  (with  $S(\omega)$  exponentially suppressed for  $\omega > \omega_c$ ). This is due to the fact that in UDD the ultra-efficient suppression of low-frequency noise is possible at the cost of actually enhancing (compared to other sequences) the influence of high-frequency noise. This is related to the existence of the sum rule for the filter function:  $\int F(\omega t)/\omega^2 d\omega = \pi t$ . In order for UDD to show a superior performance in coherence protection the timescale of interest must fulfill  $t < 2n/\omega_c$ . When this condition is not met (i.e. when the ultraviolet cutoff is irrelevant for coherence dynamics), the CPMG sequence was found to be the most efficient among the considered ones.
- For the noise with hard cutoff, and in the case of having good data at timescales  $t < 2n/\omega_c$ , one can use UDD to obtain the moments of noise spectrum:  $\chi_{\text{UDD}}(t) \sim t^{2n+2} M_{2n}$  where  $M_{2n} = \int \omega^{2n} S(\omega) d\omega$ .
- For CPMG sequence, the filter function  $F(z = \omega t)$  can be approximated at large  $n$  by a periodic train of peaks of width  $2\pi/t$ , height  $2n$ , and distance between the peaks given by  $2\pi n$ . With this observation it is easy to show that for  $S(\omega) \propto 1/\omega^\beta$  one has  $\chi(t) \propto t^{\beta+1}/n^\beta$ . This relation was later used to characterize a previously unknown noise source in an experiment on a singlet-triplet qubit [82].

Furthermore, the case of non-Gaussian Random Telegraph Noise (RTN) was considered in [H1]. Comparison of numerical simulations with theory based on Gaussian approximation showed that with increasing  $n$  the decoherence under the DD sequence becomes more similar to the prediction of a Gaussian theory (in which only the first spectral density of RTN is used). In [H1] this observation was supported by analytical calculation of the 4th cumulant of filtered RTN, i.e. the  $\chi_4$  term in expansion of  $\ln W(t) = -\chi_2(t) - \chi_4(t) + \dots$ , which showed that the ratio of  $\chi_4/\chi_2$  remains  $\ll 1$  on a timescale which is increasing faster with  $n$  than the coherence decay timescale  $T_2$  defined by  $\chi_2(T_2) = 1$ . A more intuitive explanation of this feature was later given in [H8] (see below).

As somewhat embarrassing fact should be mentioned here. As discussed above, in [H1] it was noted that the CPMG filter function in frequency space looks like a series of delta-like peaks at large  $n$ , and this feature was in fact used in calculations. However, one simple consequence of this was only noted later by other researchers [83, 84]: in many cases (especially for monotonically

decreasing  $S(\omega)$  it is enough to keep only the contribution of first of these peaks in expression for  $\chi(t)$ :

$$\chi(t) \approx \frac{4v_1^2 t}{\pi^2} S\left(\frac{\pi n}{t}\right). \quad (74)$$

This observation leads to the most practical recipe for performing real spectroscopy of  $S(\omega)$  by application of CPMG sequences, and fitting the measured coherence for various  $n$  and  $t$  to Eq. (74).

### 4.3.2 Quadratic coupling to classical Gaussian noise: qubit at the optimal working point

One often encounters the case in which the coupling to the noise is quadratic:

$$\hat{H} = \frac{1}{2}[\Omega + v_2 \xi^2(t')] \hat{\sigma}_z, \quad (75)$$

where  $\Omega$  is the controlled qubit splitting, and  $v_2$  is the coupling constant. Such a  $\hat{H}$  arises when  $\Omega$  has an extremum as a function of an external noisy parameter  $B_z(t')$ , i.e.  $\partial\Omega/\partial B_z|_{B_z=B_0}=0$ . Then, for  $B_z$  tuned to  $B_0$ , i.e. at an Optimal Working Point (OWP) of the qubit, the noise  $\xi(t') \propto B(t') - B_0$  enters quadratically into Eq. (75). If we also consider transverse noise, i.e.  $v_x \xi_x(t') \hat{\sigma}_x$  term, then for  $v_x \xi_x \ll \Omega$  we again arrive in the lowest order at Eq. (75) with  $v_2 = v_x^2/2\Omega$ . At such an OWP the influence of noise is suppressed, and the qubit dephasing time is longer than in the case of linear coupling to the noise. The theoretical challenge is posed by the fact that while  $\xi(t)$  is assumed to be a Gaussian process, its square is *not Gaussian-distributed*: the  $\xi^2(t)$  process has nontrivial correlators beyond the two-point correlation function.

Let me mention here a very interesting connection between the theory presented in this chapter and the previously discussed effective-Hamiltonian based theory of hf-induced spin qubit decoherence. The Hamiltonian given by Eq. (75) also appears when longitudinal  $\xi_z$  noise is of intrinsically low-frequency character (and thus its influence of linear term in  $\xi_z$  is completely removed by DD), while the transverse  $\xi_\perp$  noise has components at higher frequencies, and its influence is furthermore suppressed by large energy splitting  $\Omega$ . This is exactly the case for a spin qubit coupled by hyperfine interaction to a nuclear bath at finite magnetic field: as it was previously discussed, longitudinal fluctuations of the nuclear Overhauser field are much slower than its transverse fluctuations. The theory presented below can be viewed as a classical counterpart of the RDT presented before. Note that the crucial approximations of RDT (1/ $N$  approximation in the absence of nuclear spin polarization) were leading to Gaussian decoupling of nuclear spin correlators, i.e. the RDT was a theory of decoherence due to quadratic coupling to *quantum* Gaussian variable (the transverse Overhauser operator). Unsurprisingly then, the resummation of ring diagrams (or cumulants) will appear immediately below when we consider dephasing due to quadratic coupling to *classical* Gaussian process.

The decoherence function in the quadratic coupling case is given by

$$W(t) = \left\langle \exp\left(-i \int_0^t f(t') v_2 \xi^2(t') dt'\right) \right\rangle. \quad (76)$$

The average over noise can be performed using the linked-cluster (cumulant) expansion, building on seminal papers [85–87] in which free evolution dephasing at an OWP was considered. We write

$$W(t) = \exp\left(\sum_{k=2}^{\infty} \frac{(-iv_2)^k}{k} R_k(t)\right) = e^{-\sum_{k=2} \chi_k(t)}, \quad (77)$$

with the linked cluster (or ring diagram) contributions

$$R_k = 2^{k-1} \int f_t(t_1) dt_1 \dots \int f_t(t_k) dt_k C(t_{12}) \dots C(t_{k1}), \quad (78)$$

$$= 2^{k-1} \int \frac{d\omega_1 \dots d\omega_k}{(2\pi)^k} S(\omega_1) \dots S(\omega_k) \tilde{f}_t(\omega_{12}) \dots \tilde{f}_t(\omega_{k1}), \quad (79)$$

where  $t_{kl} \equiv t_k - t_l$ , and  $\omega_{kl} \equiv \omega_k - \omega_l$ . Now we have to calculate all the terms in the cumulant expansion, not only the second one, as was the case for linear coupling to Gaussian noise.

In [H8] solutions for the above problem were given in two cases. For noise with non-singular spectrum at low frequencies (i.e. noise having a well-defined autocorrelation time) it was argued that at large  $n$  the dephasing at relatively short timescales can be described using a Gaussian approximation (i.e. keeping only  $R_2(t)$  in the expansion above). The second case is that of  $1/f^\beta$  noise, for which the  $R_k$  can be resummed, provided that the quasi-static (low-frequency) noise is stronger than the high-frequency noise (which is the case for  $\beta > 1$ ).

In the first case we can give the following explanation why with increasing  $n$  the noise affecting the qubit should become better described within the Gaussian approximation. While the phase  $\phi(t) = \int_0^t \xi^2(t') dt'$  is not Gaussian-distributed except at very long  $t$ , the filtered phase,  $\phi_f(t) = \int f_t(t') \xi^2(t') dt'$ , can be viewed as a sum over  $n + 1$  contributions, with signs chosen in such a way that correlated contributions mostly cancel each other. If the correlation time of  $\xi^2(t)$  process,  $t_c$ , is finite, then for  $t/n \ll t_c \ll t$  the DD filtering suppresses the dephasing, while the correlations exist only among small subsets of contributions to  $\phi_f$ . The latter observation allows us to invoke the Central Limit Theorem, leading to Gaussian distribution of  $\phi_f$  at large  $n$ . This applies to any non-Gaussian noise with finite  $t_c$ , so it also explains in an intuitive fashion the result given in [H1], where the influence of RTN (which is non-Gaussian) was shown to be well-described by Gaussian approximation at large  $n$ .

In this approximation we have  $W(t) = e^{-\chi_2(t)}$  with

$$\chi_2(t) = v_2^2 \int_0^\infty \frac{d\omega}{2\pi} S_2(\omega) |\tilde{f}_t(\omega)|^2 \quad (80)$$

which is the same as Eq. (69), only with  $S(\omega)$  replaced by the spectral density of  $\xi^2$  process, given by

$$S_2(\omega) = \int S(\omega_1) S(\omega_1 - \omega) \frac{d\omega_1}{\pi}. \quad (81)$$

At large  $n$  one can then use Eq. (74) to perform spectroscopy of this quantity. In [H8] the accuracy of the Gaussian approximation was checked using an example of Ornstein-Uhlenbeck noise with correlation time  $t_c$ . For number of pulses  $n$ , evolution time  $t$ , and correlation time  $t_c$  fulfilling the above conditions the results of numerical simulations confirmed the accuracy of Gaussian approximation when  $t \leq T_2$ .

On the other hand, for noise with ill-defined  $t_c$ , or simply for  $t \ll t_c$  (which has to be physically indistinguishable from the former case), we can obtain a very different solution when the noise is dominated by low-frequency fluctuations. We can write then that during a single evolution, the noise contribution to qubit's splitting is  $\xi^2(t') \approx \xi_{lf}^2 + 2\xi_{lf} \delta\xi(t') + \delta\xi^2(t')$ , with  $\xi_{lf}$  being the quasi-static shift changing between measurements (i.e. coming from noise spectrum for  $\omega_0 < \omega < 1/t$ ), and with  $\delta\xi(t')$  being the high-frequency component. The low-frequency cutoff is  $\omega_0 \approx 1/T_M$ , with  $T_M$  being the total data acquisition time. Since typically  $T_M$  is orders of magnitude larger than  $t$ , for noise with spectral weight concentrated at low  $\omega$  we have  $\langle \xi_{lf}^2 \rangle \gg \langle \delta\xi^2 \rangle$ , and the dominant noisy term is  $2\xi_{lf} \delta\xi(t')$  (note that the influence of the quasi-static shift  $\xi_{lf}^2$  is removed by the DD sequence). This amounts to an observation that in the presence of  $1/f^\beta$  noise the position of the OWP is not well defined: for  $T_M \gg t$  we average over evolutions of qubits operated in the neighborhood of an OWP.

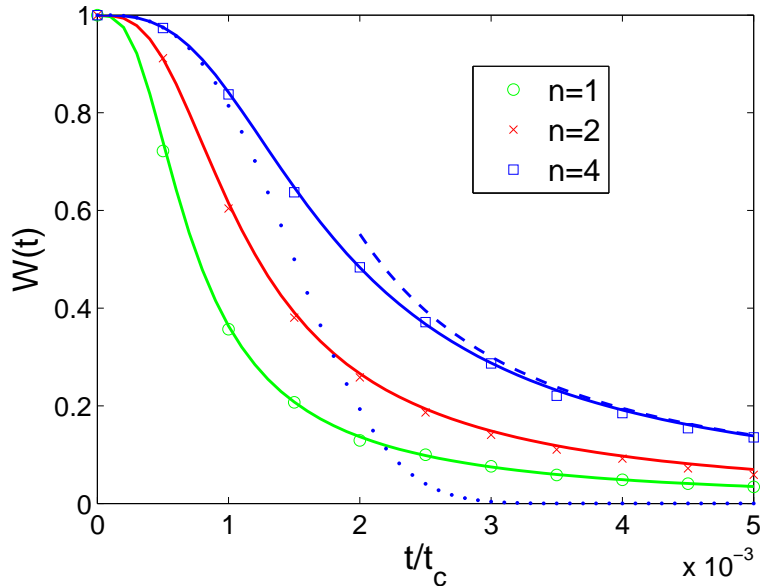


Figure 8: Decoherence due to OU noise at an OWP for CP sequence with  $n = 1, 2,$  and  $4$ . Symbols are the results of numerical simulation. For each  $t$  the averaging time was  $T_M = Mt$  with  $M = 10^6$ , so that the resulting  $\sigma_0^2$  was well approximated by the total power of the OU noise. With coupling  $v_2\sigma_0^2 = 10^5/t_c$ , the coherence decay in the presented time range is due to  $1/\omega^2$  tail of  $S(\omega)$ . The solid lines are obtained using Eq. (84). For  $n=4$  the dotted line is the Gaussian approximation, and the dashed line is  $W(t) \sim t^{-3/2}$  asymptotics from Eq. (86). The figure is adapted from [H8].

The essence of the calculation below is separate averaging over these slow and fast fluctuations. The first average is over  $\xi_{lf}$ , which is treated as a static Gaussian variable with standard deviation given by

$$\sigma_0^2 = \int_{\omega_0}^{1/t} S(\omega) d\omega / \pi \approx \frac{A_\beta}{\pi(\beta - 1)\omega_0^{\beta-1}}. \quad (82)$$

where  $S(\omega) = A_\beta/|\omega|^\beta$  with  $\beta > 1$  was used. The second average over high frequencies is also Gaussian, and it reads:

$$W(t) = \left\langle \exp \left[ -iv_2 \int f_t(t') \delta\xi^2(t') dt' - 2\sigma_0^2 v_2^2 \int dt_1 \int dt_2 f_t(t_1) f_t(t_2) \delta\xi(t_1) \delta\xi(t_2) \right] \right\rangle_{\text{hf}}. \quad (83)$$

In Eq. (83) the second term is expected to dominate when  $\sigma_0^2 \gg \langle \delta\xi^2 \rangle_{\text{hf}}$ , i.e. when  $T_M \gg t$ . The calculation of the average involving only this term can be done by coming back to Eq. (78), into which we plug in  $C(t) = \langle \delta\xi(t) \delta\xi(0) \rangle_{\text{hf}} + \sigma_0^2$ , and keep only the terms with the maximal power of  $\sigma_0$ , i.e. the ones in which every second  $C(t_{kl})$  is replaced by  $\sigma_0^2$ . The resulting sum over all  $R_k$  can be in fact performed [H8], and the result is

$$W(t) = \frac{1}{\sqrt{1 + 4v_2^2 \sigma_0^2 R_2^l(t)}}, \quad (84)$$

where  $R_2^l$  is given by the familiar formula:

$$R_2^l = \int_0^\infty |\tilde{f}_t(\omega)|^2 S(\omega) \frac{d\omega}{\pi}. \quad (85)$$

In Fig. 8 this Equation is compared with the results of numerical simulations of dephasing due to noise with  $S(\omega) \propto 1/\omega^2$  and a low-frequency cutoff at  $\omega_0 \ll 1/t$  (actually an OU noise strongly coupled to the qubit causing dephasing for  $t \ll t_c = \omega_0^{-1}$ ).

For large  $n$  we can use Eq. (74) to relate  $R_2^l(t)$  to  $S(n\pi/t)$ . When  $S(\omega \approx n\pi/t) \propto 1/\omega^\beta$  in a wide frequency range we have

$$W(t) \approx (T_2/t)^{\frac{\beta+1}{2}} \text{ for } t \gg T_2, \quad (86)$$

where the characteristic decay timescale fulfills

$$T_2 \sim n^\gamma / T_M^\eta \text{ where } \gamma = \frac{\beta}{\beta+1} \text{ and } \eta = \frac{\beta' - 1}{\beta + 1}. \quad (87)$$

These results show how the analysis of time dependence of decoherence at an OWP can be used to perform spectroscopy of  $1/f$ -type noise.

Finally, let me note that the similarity of Eq. (84) to Eq. (38) is not accidental. The result concerning the echo decay for a spin qubit interacting with a nuclear bath has a structure analogous to a square of Eq. (84) because in that case we had to average over two independent Gaussian variables ( $x$  and  $y$  components of the Overhauser field).

## References

- [1] D. J. Wineland, Rev. Mod. Phys. **85**, 1103 (2013).
- [2] S. Haroche, Rev. Mod. Phys. **85**, 1083 (2013).
- [3] W. H. Zurek, Physics Today **44**, issue 10, page 36 (1991), arXiv:quant-ph/0306072 (2003).
- [4] A. Ekert and R. Jozsa, Rev. Mod. Phys. **68**, 733 (1996).
- [5] S. J. Devitt, W. J. Munro, and K. Nemoto, Rep. Prog. Phys. **76**, 076001 (2013).
- [6] J. R. Petta, A. C. Johnson, J. M. Taylor, E. A. Laird, A. Yacoby, M. D. Lukin, C. M. Marcus, M. P. Hanson, and A. C. Gossard, Science **309**, 2180 (2005).
- [7] F. H. L. Koppens, K. C. Nowack, and L. M. K. Vandersypen, Phys. Rev. Lett. **100**, 236802 (2008).
- [8] H. Bluhm, S. Foletti, I. Neder, M. Rudner, D. Mahalu, V. Umansky, and A. Yacoby, Nat. Phys. **7**, 109 (2010).
- [9] H. Bluhm, S. Foletti, D. Mahalu, V. Umansky, and A. Yacoby, Phys. Rev. Lett. **105**, 216803 (2010).
- [10] M. D. Shulman, O. E. Dial, S. P. Harvey, H. Bluhm, V. Umansky, and A. Yacoby, Science **336**, 202 (2012).
- [11] W. A. Coish, J. Fischer, and D. Loss, Phys. Rev. B **77**, 125329 (2008).
- [12] W. A. Coish, J. Fischer, and D. Loss, Phys. Rev. B **81**, 165315 (2010).
- [13] D. Loss and D. P. DiVincenzo, Phys. Rev. A **57**, 120 (1998).
- [14] R. Hanson, L. P. Kouwenhoven, J. R. Petta, S. Tarucha, and L. M. K. Vandersypen, Rev. Mod. Phys. **79**, 1217 (2007).
- [15] R.-B. Liu, W. Yao, and L. J. Sham, Adv. Phys. **59**, 703 (2010).
- [16] K. De Greve, D. Press, P. L. McMahon, and Y. Yamamoto, Rep. Prog. Phys. **76**, 092501 (2013).

- [17] A. V. Khaetskii and Y. V. Nazarov, Phys. Rev. B **64**, 125316 (2001).
- [18] M. Kroutvar, Y. Ducommun, D. Heiss, M. Bichler, D. Schuh, G. Abstreiter, and J. J. Finley, Nature **432**, 81 (2004).
- [19] J. M. Elzerman, R. Hanson, L. H. Willems van Beveren, B. Witkamp, L. M. K. Vandersypen, and L. P. Kouwenhoven, Nature **430**, 431 (2004).
- [20] K. Blum, *Density Matrix Theory and Applications* (Plenum Press, New York, 1981).
- [21] V. N. Golovach, A. Khaetskii, and D. Loss, Phys. Rev. Lett. **93**, 016601 (2004).
- [22] I. A. Merkulov, A. L. Efros, and M. Rosen, Phys. Rev. B **65**, 205309 (2002).
- [23] V. V. Dobrovitski, H. A. De Raedt, M. I. Katsnelson, and B. N. Harmon, arXiv:quant-ph/0112053 (2001).
- [24] A. V. Khaetskii, D. Loss, and L. Glazman, Phys. Rev. Lett. **88**, 186802 (2002).
- [25] O. E. Dial, M. D. Shulman, S. P. Harvey, H. Bluhm, V. Umansky, and A. Yacoby, Phys. Rev. Lett. **110**, 146804 (2013).
- [26] M. Gaudin, J. Phys. (France) **37**, 1087 (1976).
- [27] M. Bortz, S. Eggert, C. Schneider, R. Stübner, and J. Stolze, Phys. Rev. B **82**, 161308 (2010).
- [28] A. Faribault and D. Schuricht, Phys. Rev. Lett. **110**, 040405 (2013).
- [29] W. Zhang, N. Konstantinidis, K. A. Al-Hassanieh, and V. V. Dobrovitski, J. Phys.:Condens. Matter **19**, 083202 (2007).
- [30] A. Abragam, *The Principles of Nuclear Magnetism* (Oxford University Press, New York, 1983).
- [31] A. Greilich, A. Shabaev, D. R. Yakovlev, A. L. Efros, I. A. Yugova, D. Reuter, A. D. Wieck, and M. Bayer, Science **317**, 1896 (2007).
- [32] D. J. Reilly, J. M. Taylor, E. A. Laird, J. R. Petta, C. M. Marcus, M. P. Hanson, and A. C. Gossard, Phys. Rev. Lett. **101**, 236803 (2008).
- [33] C. Deng and X. Hu, Phys. Rev. B **72**, 165333 (2005).
- [34] J. Rammer, *Quantum Field Theory of Non-equilibrium States* (Cambridge University Press, New York, 2007).
- [35] A. Greilich, D. R. Yakovlev, A. Shabaev, A. L. Efros, I. A. Yugova, R. Oulton, V. Stavarache, D. Reuter, A. Wieck, and M. Bayer, Science **313**, 341 (2006).
- [36] A. Greilich, S. E. Economou, S. Spatzek, D. R. Yakovlev, D. Reuter, A. D. Wieck, T. L. Reinecke, and M. Bayer, Nat. Phys. **5**, 262 (2009).
- [37] P.-F. Braun, X. Marie, L. Lombez, B. Urbaszek, T. Amand, P. Renucci, V. K. Kalevich, K. V. Kavokin, O. Krebs, P. Voisin, and Y. Masumoto, Phys. Rev. Lett. **94**, 116601 (2005).
- [38] M. V. Gurudev Dutt, J. Cheng, B. Li, X. Xu, X. Li, P. R. Berman, D. G. Steel, A. S. Bracker, D. Gammon, S. E. Economou, R.-B. Liu, and L. J. Sham, Phys. Rev. Lett. **94**, 227403 (2005).

- [39] F. H. L. Koppens, J. A. Folk, J. M. Elzerman, R. Hanson, L. H. W. van Beveren, I. T. Vink, H. P. Tranitz, W. Wegscheider, L. P. Kouwenhoven, and L. M. K. Vandersypen, *Science* **309**, 1346 (2005).
- [40] A. C. Johnson, J. R. Petta, J. M. Taylor, A. Yacoby, M. D. Lukin, C. M. Marcus, M. P. Hanson, and A. C. Gossard, *Nature* **435**, 925 (2005).
- [41] D. J. Reilly, C. M. Marcus, M. P. Hanson, and A. C. Gossard, *Appl. Phys. Lett.* **91**, 162101 (2007).
- [42] E. L. Hahn, *Phys. Rev.* **80**, 580 (1950).
- [43] U. Haeblerlen, *High Resolution NMR in Solids, Advances in Magnetic Resonance Series, Supplement 1* (Academic, New York, 1976).
- [44] L. Viola and S. Lloyd, *Phys. Rev. A* **58**, 2733 (1998).
- [45] K. Khodjasteh and D. A. Lidar, *Phys. Rev. A* **75**, 062310 (2007).
- [46] G. S. Uhrig, *Phys. Rev. Lett.* **98**, 100504 (2007).
- [47] D. Klauser, W. A. Coish, and D. Loss, *Phys. Rev. B* **73**, 205302 (2006).
- [48] G. Giedke, J. M. Taylor, D. D'Alessandro, M. D. Lukin, and A. Imamoglu, *Phys. Rev. A* **74**, 032316 (2006).
- [49] D. Stepanenko, G. Burkard, G. Giedke, and A. Imamoglu, *Phys. Rev. Lett.* **96**, 136401 (2006).
- [50] C. Barthel, D. J. Reilly, C. M. Marcus, M. P. Hanson, and A. C. Gossard, *Phys. Rev. Lett.* **103**, 160503 (2009).
- [51] R. Kubo, *J. Phys. Soc. Jpn.* **17**, 1100 (1962).
- [52] S. K. Saikin, W. Yao, and L. J. Sham, *Phys. Rev. B* **75**, 125314 (2007).
- [53] W. Yang and R.-B. Liu, *Phys. Rev. B* **78**, 085315 (2008).
- [54] W. M. Witzel and S. Das Sarma, *Phys. Rev. B* **74**, 035322 (2006).
- [55] W. M. Witzel, R. de Sousa, and S. Das Sarma, *Phys. Rev. B* **72**, 161306(R) (2005).
- [56] W. Yao, R.-B. Liu, and L. J. Sham, *Phys. Rev. B* **74**, 195301 (2006).
- [57] W. M. Witzel and S. Das Sarma, *Phys. Rev. B* **77**, 165319 (2008).
- [58] W. M. Witzel and S. Das Sarma, *Phys. Rev. Lett.* **98**, 077601 (2007).
- [59] B. Lee, W. M. Witzel, and S. Das Sarma, *Phys. Rev. Lett.* **100**, 160505 (2008).
- [60] A. M. Tyryshkin, J. J. L. Morton, S. C. Benjamin, A. Ardavan, G. A. D. Briggs, J. W. Ager, and S. A. Lyon, *J. Phys. Condens. Matter* **18**, S783 (2006).
- [61] E. Abe, A. M. Tyryshkin, S. Tojo, J. J. L. Morton, W. M. Witzel, A. Fujimoto, J. W. Ager, E. E. Haller, J. Isoya, S. A. Lyon, M. L. W. Thewalt, and K. M. Itoh, *Phys. Rev. B* **82**, 121201 (2010).
- [62] N. Shenvi, R. de Sousa, and K. B. Whaley, *Phys. Rev. B* **71**, 224411 (2005).
- [63] R. Brout, *Phys. Rev.* **118**, 1009 (1960).

- [64] I. Neder, M. S. Rudner, H. Bluhm, S. Foletti, B. I. Halperin, and A. Yacoby, *Phys. Rev. B* **84**, 035441 (2011).
- [65] W. B. Mims, *Phys. Rev. B* **5**, 2409 (1972).
- [66] S. Saikin and L. Fedichkin, *Phys. Rev. B* **67**, 161302(R) (2003).
- [67] W. M. Witzel, X. Hu, and S. Das Sarma, *Phys. Rev. B* **76**, 035212 (2007).
- [68] F. T. Arecchi, E. Courtens, R. Gilmore, and H. Thomas, *Phys. Rev. A* **6**, 2211 (1972).
- [69] A. Melikidze, V. V. Dobrovitski, H. A. De Raedt, M. I. Katsnelson, and B. N. Harmon, *Phys. Rev. B* **70**, 014435 (2004).
- [70] S. Foletti, H. Bluhm, D. Mahalu, V. Umansky, and A. Yacoby, *Nat. Phys.* **5**, 903 (2009).
- [71] A. P. Higginbotham, F. Kuemmeth, M. P. Hanson, A. C. Gossard, and C. M. Marcus, *Phys. Rev. Lett.* **112**, 026801 (2014).
- [72] W. A. Coish and D. Loss, *Phys. Rev. B* **72**, 125337 (2005).
- [73] J. M. Taylor, J. R. Petta, A. C. Johnson, A. Yacoby, C. M. Marcus, and M. D. Lukin, *Phys. Rev. B* **76**, 035315 (2007).
- [74] W. A. Coish and D. Loss, *Phys. Rev. B* **70**, 195340 (2004).
- [75] E. Fick and G. Saueremann, *The Quantum Statistics of Dynamics Processes* (Springer Verlag, Berlin Heidelberg, 1990).
- [76] H. Breuer and F. Petruccione, *The Theory of Open Quantum Systems* (Oxford University Press, Oxford, 2007).
- [77] J. Fischer and H.-P. Breuer, *Phys. Rev. A* **76**, 052119 (2007).
- [78] E. Ferraro, H.-P. Breuer, A. Napoli, M. A. Jivulescu, and A. Messina, *Phys. Rev. B* **78**, 064309 (2008).
- [79] E. Barnes, Ł. Cywiński, and S. Das Sarma, *Phys. Rev. Lett.* **109**, 140403 (2012).
- [80] R. J. Schoelkopf, A. A. Clerk, S. M. Girvin, K. W. Lehnert, and M. H. Devoret, in *Quantum Noise in Mesoscopic Physics*, edited by Y. V. Nazarov (Kluwer, Dordrecht, 2003) pp. 175–203, (cond-mat/0210247).
- [81] R. de Sousa, *Top. Appl. Phys.* **115**, 183 (2009).
- [82] J. Medford, Ł. Cywiński, C. Barthel, C. M. Marcus, M. P. Hanson, and A. C. Gossard, *Phys. Rev. Lett.* **108**, 086802 (2012).
- [83] J. Bylander, S. Gustavsson, F. Yan, F. Yoshihara, K. Harrabi, G. Fitch, D. G. Cory, Y. Nakamura, J.-S. Tsai, and W. D. Oliver, *Nat. Phys.* **7**, 565 (2011).
- [84] G. A. Álvarez and D. Suter, *Phys. Rev. Lett.* **107**, 230501 (2011).
- [85] Y. Makhlin and A. Shnirman, *Phys. Rev. Lett.* **92**, 178301 (2004).
- [86] Y. Makhlin, G. Schön, and A. Shnirman, *Chem. Phys.* **296**, 315 (2004).
- [87] G. Falci, A. D'Arrigo, A. Mastellone, and E. Paladino, *Phys. Rev. Lett.* **94**, 167002 (2005).
- [88] A. M. Tyryshkin, S. Tojo, J. J. L. Morton, H. Riemann, N. V. Abrosimov, P. Becker, H.-J. Pohl, T. Schenkel, M. L. W. Thewalt, K. M. Itoh, and S. A. Lyon, *Nat. Materials* **11**, 143 (2012).

## 5 Description of other scientific achievements

### a) Bibliometric data (from October 20th, 2014)

Number of published scientific papers: 34

Citations with autocitations excluded: 929 (according to Web of Science)

Cumulative impact factor: 150.47

H-index: 17 (according to Web of Sciece)

### b) Research not included in the habilitation thesis

### 5.1 Research done before obtaining the PhD title

While earning my Master's degree at the Warsaw University, working under supervision of professor Witold Bardyszewski, I have developed a theory of light absorption in disordered semiconductors, with special focus on the absorption in heavily-disordered p-type materials such as GaMnAs. Elements of this theory were later used in the paper:

K. Dziatkowski, Ł. Cywiński, W. Bardyszewski, A. Twardowski, H. Saito, and K. Ando, *Influence of disorder on the optical absorption in semiconductors: Application to epitaxially grown III-V compounds*, Phys. Rev. B **73**, 235340 (2006).

During my graduate studies at UCSD I worked on two topics: (1) non-equilibrium electron dynamics and ultrafast light-induced demagnetization in ferromagnetic semiconductors and metals, and (2) spin diffusion in planar metal-semiconductor structures with applications for possible spintronic devices.

Research on topic (1) was done in collaboration with an experimental group of professor Junichiro Kono from Rice University in Texas. I have developed a theoretical model of ultrafast decay of magnetization caused by strong photoexcitation in (III,Mn)V magnetic semiconductors. The papers [D1,D2,D4] were the result of this collaboration. Paper [D3] contains a detailed description of theory of light-induced demagnetization in materials in which the sp-d model of ferromagnetism is applicable.

The research on topic (2) was done in close collaboration with dr Hanan Dery, who was a postdoc working with my advisor. We have worked together on theory of spin transport in realistic structures consisting of iron and GaAs, with special attention devoted to possible spintronic devices based on such structures. In [D5] we presented an easy to use theory of spin diffusion in layered structures of magnetic metals and semiconductors, which we latter applied in our investigations of multi-terminal spintronic devices: a three-terminal spin transistor [D6], a device converting the circular polarization of absorbed light into an electrical signal [D7], a three-terminal system in which magnetization dynamics of one of the ferromagnetic electrodes is sensed electrically [D8], and a five-terminal reprogrammable logic gate [D9]. An invited review [D10] summarized these works.

[D1] J. Wang, C. Sun, J. Kono, A. Oiwa, H. Munekata, Ł. Cywiński and L.J. Sham, *Ultrafast Quenching of Ferromagnetism in InMnAs Induced by Intense Laser Irradiation*, Phys. Rev. Lett. **95**, 167401 (2005).

[D2] J. Wang, C. Sun, Y. Hashimoto, J. Kono, G.A. Khodaparast, Ł. Cywiński, L.J. Sham, G.D. Sanders, C.J. Stanton, H. Munekata, *Ultrafast Magneto-Optics in Ferromagnetic III-V Semiconductors*, J. Phys.: Condens. Matter **18**, R501 (2006).

[D3] Ł. Cywiński and L.J. Sham, *Ultrafast demagnetization in the sp-d model: a theoretical study*, Phys. Rev. B **76**, 045205 (2007).

- [D4] J. Wang, Ł. Cywiński, C. Sun, J. Kono, H. Mune-kata, and L.J. Sham, *Femtosecond demagnetization and hot hole relaxation in ferromagnetic GaMnAs*, Phys. Rev. B **77**, 235308 (2008).
- [D5] H. Dery, Ł. Cywiński and L.J. Sham, *Lateral diffusive spin transport in layered structures*, Phys. Rev. B **73**, 041306(R) (2006).
- [D6] H. Dery, Ł. Cywiński, and L.J. Sham, *Spin transference and magnetoresistance amplification in a transistor*, Phys. Rev. B **73**, 161307(R) (2006).
- [D7] H. Dery, Ł. Cywiński, and L.J. Sham, *Spintronics for electrical measurement of light polarization*, J. Appl. Phys. **100**, 063713 (2006).
- [D8] Ł. Cywiński, H. Dery, and L.J. Sham, *Electric readout of magnetization dynamics in a ferromagnet-semiconductor system*, Appl. Phys. Lett. **89**, 042105 (2006).
- [D9] H. Dery, P. Dalal, Ł. Cywiński, and L.J. Sham, *Spin based logic in semiconductors for reconfigurable large scale circuits*, Nature **447**, 573 (2007).
- [D10] Ł. Cywiński, H. Dery, P. Dalal, and L.J. Sham, *Electrical expression of spin accumulation in ferromagnet/semiconductor structures*, Mod. Phys. Lett. B **21**, 1509 (2007).

## 5.2 Research done after obtaining the PhD title: works closely related to the topic of this thesis

Five papers below are quite closely related to the topic of this thesis, but they are not included in the main cycle of papers, since I cannot claim to be a leading author of them.

In [A1] we considered a specific model of fermionic bath causing dephasing of superconducting qubits: a bath of so-called Andreev fluctuators. Such a bath consists of many carrier trapping centers localized in an insulating material in the proximity to the superconductor. Pairs of centers become charged and discharged due to transfer of Cooper pairs between the condensate and the insulator. The resulting charge noise causes pure dephasing of a superconducting qubit of the Cooper pair-box type. In this paper we used the Keldysh technique to derive the decoherence function  $W(t)$  for any possible sequence of pulses affecting the qubit, and linked-cluster expansion of the second order was employed. At this level of approximation it was possible to map the interaction with the bath on interaction with noise having spectral density closely approximated by  $1/f$  form.

Paper [A2] is an experimental work on dynamical decoupling of a singlet-triplet qubit made of a GaAs double quantum dot. Using methods of [H1] (with some further improvements specific to the case of  $1/\omega^\beta$  noise with  $\beta > 2$ ) I was able to reconstruct the spectral density of noise from the CPMG results with  $n=2, 4, 8, 16$ , and  $32$  pulses. The reconstructed  $S(\omega) \propto 1/\omega^{2.6}$  allowed for succesful prediction of decay timescale for the spin echo ( $n=1$ ) and the CPMG sequence with  $n=3$ .

In [A3] we have used the insights from [H6], and we applied the time-convolutionless master equation technique to the NFID problem. Starting from the full hf Hamiltonian we re-derived the RDT result at short times and zero bath polarizations, and we obtained a nontrivial generalization of this result to the case of polarized nuclear bath. A new, previously never discussed in the literature, kind of oscillations, appearing in NFID signal for large bath polarization, was predicted there.

In papers [A4,A5] a real-space cluster expansion technique was used to calculate the coherence decay of an electron spin coupled to a spin bath consisting of spins of other electrons. This is the case in which the inter-bath coupling is of the same strength as the qubit-bath coupling, which necessitates consideration of large clusters of spins. Proper averaging over many states of the bath is also more complicated than in the previously considered case in which the qubit-bath

coupling was dominating over the intrabath couplings: now many bath spins have a nontrivial influence on dynamics of a few-spin cluster, since the dipolar interactions with these “outside” spins strongly influence the energy splittings of the spins within the cluster. In [A4] the spin echo decoherence of electrons bound to phosphorous donors in silicon was considered, and the nontrivial dependence of the  $T_2$  time on the concentration of both the electronic spins and the nuclear spins was predicted (this prediction was later confirmed in experiments [88]). In [A5] we described the theory in more detail, and gave more predictions for both donors in Si and NV centers in diamond.

- [A1] R.M. Lutchyn, Ł. Cywiński, C.P. Nave, and S. Das Sarma, *Quantum decoherence of a charge qubit in a spin-fermion model*, Phys. Rev. B **78**, 024508 (2008).
- [A2] J. Medford, Ł. Cywiński, C. Barthel, C.M. Marcus, M.P. Hanson, and A.C. Gossard, *Scaling of Dynamical Decoupling for Spin Qubits*, Phys. Rev. Lett. **108**, 086802 (2012).
- [A3] E. Barnes, Ł. Cywiński, and S. Das Sarma, *Nonperturbative Master Equation Solution of Central Spin Dephasing Dynamics*, Phys. Rev. Lett. **109**, 140403 (2012).
- [A4] W.M. Witzel, M.S. Carroll, A. Morello, Ł. Cywiński, and S. Das Sarma, *Electron spin decoherence in isotope-enriched silicon*, Phys. Rev. Lett. **105**, 187602 (2010).
- [A5] W.M. Witzel, M.S. Carroll, Ł. Cywiński, and S. Das Sarma, *Quantum Decoherence of the Central Spin in a Sparse System of Dipolar Coupled Spins*, Phys. Rev. B **86**, 035452 (2012).

### 5.3 Research done after obtaining the PhD title: works on other topics

In 2009-2010 I worked on theory of silicon double quantum dots. We analyzed how the multi-valley structure of the bottom of conduction band in Si affects the performance of singlet-triplet qubits [Si1,Si2], and we calculated the dependence of exchange coupling on parameters of the two dots [Si3].

- [Si1] D. Culcer, Ł. Cywiński, Q.Z. Li, X. Hu, and S. Das Sarma, *Realizing singlet-triplet qubits in multivalley Si quantum dots*, Phys. Rev. B **80**, 205302 (2009).
- [Si2] D. Culcer, Ł. Cywiński, Q.Z. Li, X. Hu, and S. Das Sarma, *Quantum dot spin qubits in Silicon: Multivalley physics*, Phys. Rev. B **82**, 155312 (2010).
- [Si3] Q.Z. Li, Ł. Cywiński, D. Culcer, X. Hu, and S. Das Sarma, *Exchange coupling in silicon quantum dots: theoretical considerations for quantum computation*, Phys. Rev. B **81**, 085313 (2010).

Starting from 2010 I have also been involved in research on CdTe self-assembled quantum dots doped with Mn ions. In [Mn1] I proposed a theory of optical orientation of a single Mn spin localized in an optically excited dot. I have also participated in theoretical interpretation of experiments on dynamics of many Mn spins in a nonresonantly excited quantum dot [Mn2,Mn3].

- [Mn1] Ł. Cywiński, *Optical orientation of a single Mn spin in a quantum dot: Role of carrier spin relaxation*, Phys. Rev. B **82**, 075321 (2010).
- [Mn2] Ł. Kłopotowski, Ł. Cywiński, P. Wojnar, V. Voliotis, K. Fronc, T. Kazimierzczuk, A. Golnik, M. Ravaro, R. Grousson, G. Karczewski, and T. Wojtowicz, *Magnetic polaron formation and exciton spin relaxation in single  $Cd_{1-x}Mn_xTe$  quantum dots*, Phys. Rev. B **83**, 081306(R) (2011).

[Mn3] Ł. Kłopotowski, Ł. Cywiński, M. Szymura, V. Voliotis, R. Grousson, P. Wojnar K. Fronc, T. Kazimierzczuk, A. Golnik, G. Karczewski, and T. Wojtowicz, *Influence of exciton spin relaxation on the photoluminescence spectra of semimagnetic quantum dots*, Phys. Rev. B **87**, 245316 (2013).

I have also provided some theoretical help in experimental work on recombination of “dark” excitons in CdTe quantum dots free of Mn ions (in which the nominally optically inactive states actually couple to light due to the presence of heavy-light hole mixing).

[X1] T. Smoleński, T. Kazimierzczuk, M. Goryca, T. Jakubczyk, Ł. Kłopotowski, Ł. Cywiński, P. Wojnar, A. Golnik, and P. Kossacki, *Radiative lifetime of dark excitons in self-assembled quantum dots*, Phys. Rev. B **86**, 241305(R) (2012).

Starting from 2011 I have also spent a part of my time doing research on topological insulators (essentially a subclass of narrow-gap semiconductors exhibiting band inversion caused by strong relativistic corrections to the band structure). In [TI1] we theoretically proposed how the bandstructure characteristic for a strong topological insulator can be created in a heterostructure of PbTe and PbSnTe. In experimental works [TI2, TI3] I have contributed to the analysis of the results and their interpretation. More interesting of the two is [TI3], where we proposed a consistent interpretation of nonlocal transport measurements in a two-dimensional topological insulator.

[TI1] R. Buczko and Ł. Cywiński, *PbTe/PbSnTe heterostructures as analogs of topological insulators*, Phys. Rev. B **85**, 205319 (2012).

[TI2] K.A. Kolwas, G. Grabecki, S. Trushkin, J. Wróbel, M. Aleszkiewicz, Ł. Cywiński, T. Dietl, G. Springholz, and G. Bauer, *Absence of nonlocal resistance in microstructures of PbTe quantum wells*, Phys. Status Solidi B **250**, 37 (2013).

[TI3] G. Grabecki, J. Wróbel, M. Czapkiewicz, Ł. Cywiński, S. Gieraltowska, E. Guziewicz, M. Zhouludev, V. Gavrilenko, N. N. Mikhailov, S. A. Dvoretzki, F. Teppe, W. Knap, and T. Dietl, *Nonlocal resistance and its fluctuations in microstructures of band-inverted HgTe/(Hg, Cd)Te quantum wells*, Phys. Rev. B **88**, 165309 (2013).

#### c) awards

- 2013, Stefan Pieńkowski award of the Polish Academy of Sciences in the field of Physics and Astronomy.
- 2012, Ministry of Science and Higher Education fellowship for an outstanding young researcher for years 2012-2015.
- 2001, Leonard Sosnowski prize awarded for “Outstanding student in Solid State Physics”.

#### d) Principal Investigator in the following grants

- 08/2013–: OPUS IV grant of the Polish National Science Center (NCN). Title: *Dynamics of entanglement of localized spins in semiconductors with application to environmental noise spectroscopy*
- 01/2011-12/2011: Iuventus Plus grant of the Polish Ministry of Science and Education. Title: *Izolatory topologiczne oparte na heterostrukturach p"o"lprzewodnik"ow IV-VI (Topological insulators based on heterostructures of IV-VI semiconductors)*.

- 10/2009–11/2012: Homing grant/award for returning researcher of the Foundation for Polish Science. Title: *Spin in semiconductor nanostructures: ferromagnetism in semiconductors with nano-scale magnetic inhomogeneities and coherent properties of single spins in quantum dots*.

#### e) Participation in research projects

- European Union Innovative Economy Grant No. POIG.01.03.01-00-159/08, “InTechFun” (2009-2011).
- ERC Advanced Grant “FunDMS” (“*Functionalization of Diluted Magnetic Semiconductors*”) (2009-2011).
- Grant of the Polish National Science Center (NCN). Title: *Magnetic quantum dot molecules with CdMnTe quantum dots* (2012-2014).

#### f) Invited talks at conferences

1. Talk at Quantum Technologies Conference V in Kraków, September 7th-12th 2014. Title: “*Spectroscopy of environmental noise via measurement of decoherence of qubits*”.
2. Talk at the 42nd General Meeting of Polish Physicists in Poznań, 8th-13th September 2013. Title: “*Dekoherencja spinu elektronu oddziałuj"acego ze spinami j"adrowymi w kropce kwantowej*”.
3. Talk at the 2nd Polish-German workshop on the optical properties of nanostructures, Münster, March 14th-16th 2012. Title: “*Theory of optical orientation of a single Mn spin in a CdTe quantum dot: resonant vs nonresonant excitation*”.
4. Talk at the 17th International Winterschool on New Developments in Solid State Physics “Mauterndorf 2012”, Mauterndorf, Austria, February 12th-17th 2012. Title: “*Spin echo decay of semiconductor spin qubits*”.
5. Talk at the Joint Polish-Japanese Workshop “Spintronics - from new materials to applications”, Warsaw, November 15th-18th 2011. Title: “*Decoherence in a sparse system of dipolarly coupled spins: application to isotope-enriched silicon*”.
6. Invited talk at the 39th International School and Conference on the Physics of Semiconductors “Jaszowiec”, Krynica, June 2010. Title: “*Dephasing of electron spin qubits due to their interaction with nuclei in quantum dots*”.
7. Invited talk at the APS March Meeting 2010 in Portland, March 15th 2010. Title: “*Electron spin dephasing by hyperfine interaction with nuclei in quantum dots*”.
8. Talk at the Canada-Japan-Poland International Symposium on Semiconductor, Magnetic, and Photonic Nanostructures, Wrocław, October 5th-7th, 2009. Title: “*Pure dephasing of the spin of the electron confined in a quantum dot: the role of hyperfine-mediated interactions*”.
9. Talk at the Spintronic Device Round Table panel session at 5th International School and Conference on Spintronics and Quantum Information Technology (Spintech), Kraków, July 2009. Title: “*Spin logic in hybrid structures*”.
10. Invited talk at the APS March Meeting 2008 in New Orleans, March 10th 2008. Title: “*Ultrafast Photoinduced Demagnetization in (III,Mn)V Ferromagnetic Semiconductors*”.

### g) Collaborations with international and Polish institutions

- *Rice University, Houston, Texas (USA)* - collaboration with prof. Junichiro Kono and his PhD student Jigang Wang concerning the dynamics of optically induced ultrafast demagnetization in InMnAs and GaMnAs. This collaboration resulted in publications [D1,D2,D4].
- *Ames Laboratory (USA)* - collaboration with prof. V.V. Dobrovitski concerning modeling of spin qubit echo signal decay in low magnetic field. This collaboration resulted in publication [H4].
- *Sandia National Laboratories (USA)* - collaboration with dr Wayne Witzel concerning theory of decoherence of an electron spin qubit interacting with an electron spin bath. This collaboration resulted in publications [A4,A5].
- *Condensed Matter Theory Center, University of Maryland at College Park (USA)* - collaboration with prof. Sankar Das Sarma and dr. Edwin Barnes concerning decoherence of spin qubits. This collaboration resulted in publications [H6,A3].
- *Institute of Physics, Polish Academy of Sciences* - collaboration with dr. Łukasz Kłopotowski concerning research on dynamics of exciton spin and the spins of Mn ions in CdMnTe quantum dots. This collaboration resulted in publications [Mn2,Mn3].
- *Institute of Physics, Polish Academy of Sciences* - collaboration with prof. Ryszard Buczek concerning theory of topological insulators. This collaboration resulted in publication [TI1].
- *Institute of Experimental Physics, Faculty of Physics, University of Warsaw* - collaboration with Tomasz Smoleński and prof. Piotr Kossacki concerning research on photoorientation dynamics of Mn spins and optical activity of dark excitons in CdTe quantum dots. This collaboration resulted in publication [X1].
- *Harvard University (USA)* - collaboration with prof. C. M. Marcus and his PhD student J. Medford concerning noise spectroscopy in double quantum dots based on GaAs. This collaboration resulted in publication [A2].
- *University at Buffalo, SUNY (USA)* - collaboration with prof. Xuedong Hu and his PhD student Jo-Tzu Hung concerning theory of decoherence of singlet-triplet qubits in double quantum dots. This collaboration resulted in publication [H7].
- *Institute of Physics, Polish Academy of Sciences* - collaboration with professors G. Grabecki, J. Wróbel, and T. Dietl concerning research on transport properties of two-dimensional topological insulator realized in a quantum well of HgTe/CdHgTe, and on transport properties of PbTe/PbEuTe quantum wells. This collaboration resulted in publications [TI2] and [TI3].
- *Institute of Physics, Wrocław University of Technology* - collaboration with dr. K. Roszak concerning theory of entanglement dynamics of a few spin qubits interacting with nuclear baths.
- *Institute of Theoretical Physics, Faculty of Physics, University of Warsaw* - collaboration with P. Szańkowski and prof. M. Trippenbach concerning theory of entanglement decay of two qubits interacting with a source of classical noise.

*Sulhan Gyumh*